Padé-Borel reconstruction of the Euler-Heisenberg Lagrangian

MS-Thesis

Submitted to Indian Institute of Science Education and Research Pune in partial fulfilment of the requirements for the BS-MS Dual Degree Programme

Author: Drishti Gupta*

Supervisor: Dr. Arun M. Thalapillil*

Department of Physics

Indian Institute of Science Education and Research Pune

April 28, 2024

** Indian Institute of Science Education and Research Pune, Homi Bhabha Road, Pashan, Pune 411008, India.*

Certificate

This is to certify that this dissertation entitled "Padé-Borel reconstruction of the Euler-Heisenberg Lagrangian" towards the partial fulfilment of the BS-MS dual degree programme at the Indian Institute of Science Education and Research, Pune represents study/work carried out by Drishti Gupta at IISER Pune under the supervision of Dr. Arun M. Thalapillil, Professor in the Department of Physics at IISER Pune, during the academic year 2023-2024.

Drishti

Drishti Gupta
(student)

Dr. Arun M. Thalapillil
(supervisor)

Supervisor: Dr. Arun M. Thalapillil

Expert TAC member: Dr. Sachin Jain

Declaration

I hereby declare that the matter embodied in the report entitled "Padé-Borel reconstruction of the Euler-Heisenberg Lagrangian" are the results of the work carried out by me at the Department of Physics, Indian Institute of Science Education and Research Pune, under the supervision of Dr. Arun M. Thalapillil and the same has not been submitted elsewhere for any other degree. Wherever others contribute, every effort is made to indicate this clearly, with due reference to the literature and acknowledgement of collaborative research and discussions.

Drishti

Drishti Gupta
Roll no. 20191108

Acknowledgments

I would like to thank Dr. Thalapillil to provide me with the opportunity to work on the upcoming and rather intriguing endeavour of Resurgence for my Master's thesis, and for his incredible support and guidance throughout my journey. I also thank Dr. Jain for his support as my Expert TAC member, and for his patience while listening to my ideas regarding the project and his inputs thereafter.

I would also like to acknowledge the financial support of the INSPIRE scholarship, provided by the Department of Science and Technology, Government of India.

I am greatly indebted to my family and friends for their invaluable love and sympathy, in both good times and bad. I would not be here, presenting my thesis, without their support.

Contents

List of Figures

List of Tables

Abstract

In this thesis, we have studied the methods of Resurgence and Padé-Borel reconstruction for the one-field Euler-Heisenberg Lagrangian in the context of scalar quantum electrodynamics upto the order of one and two loops, and for the two-field Euler-Heisenberg Lagrangian in the context of quantum electrodynamics upto one loop. Both of these applications of Padé-Borel reconstructions have been largely unexamined in literature. We have derived the form of the two-field Euler-Heisenberg Lagrangian for sQED from first principles upto the order of two loops. By the means of Padé-Borel reconstruction strategies, we have constructed remarkably accurate functional approximations to the Euler-Heisenberg Lagrangian using very limited amount of perturbative data. We have been able to predict the behaviour of this function in the non-perturbative strong field regime using these approximations and other methods developed in the program of Resurgence. In our analysis, we have drawn parallels between our work and the literature already present on this subject in the case of the quantum electrodynamics Euler-Heisenberg Lagrangian, as well as pointed out new resurgent structures that had not been studied extensively in the literature.

1 Introduction

Since the advent of the quantum theory, there have been many efforts towards understanding the mathematical nature and the physical implications of different models of quantum mechanical and quantum field theories. In most cases, while it is not possible to find an exact solution for the physically relevant observables $\mathscr{O}$ in the theory, it is possible to find a perturbative expansion for small values of the coupling parameter g such that

$$\mathscr{O}(g) \stackrel{?}{=} \sum_{k\geq 0} c_k^{(0)} g^k \, . \tag{1}$$

This perturbative expansion can only be used in a domain in which this sum containing infinite number of terms is convergent. This domain of convergence is usually characterized by the radius of convergence R. However, for a large subset of quantum theories the perturbative series is seen to diverge for all domains, i.e., $R = 0$ [1, 2]. However, it turns out that this series is actually "asymptotic" to the original function $\mathscr{O}$ (see [1] for a precise mathematical definition of asymptotic series and functions). Dyson, in his seminal paper [3], argued that this apparent divergence of perturbative expansions can be attributed to some instability in some sector of the quantum theory.

However, the question of how to extract information about the underlying quantum theory using just the perturbative expansion in eq. (1) still remains. This question was answered by Écalle in his three volumes of works on the theory he coined as "Resurgence" [4–6]. Simply put, the idea of Resurgence dictates that divergences in the perturbative coefficients of an asymptotic expansion, rather than being problematic, actually contain important information about the behaviour of the underlying function $\mathscr{O}$ in the non-perturbative sector.

One method of extracting the non-perturbative information that is hidden in asymptotic series was given in 1899 to sum asymptotic series of the "Gevrey-1 type" known as "Borel summation" [7, 8]. The Gevrey-1 type asymptotic series have coefficients c_k with divergences of the form $c_k \sim A^{-k} k!$, which immediately implies $R = 0$. Using Borel summation and Resurgence techniques reveals that the perturbative series in eq. (1) of the Gevrey-1 type actually has a hidden non-perturbative part of the form $\sim e^{-A/g}$ that cannot be expanded perturbatively. Adding these non-perturbative parts to eq. (1) gives a more accurate description of the function $\mathscr{O}$ in terms of the "trans-series" written as [9]

$$\mathscr{O}(g) = \sum_{k\geq 0} c_k^{(0)} g^k + \sum_{I\geq 1} \exp\left[-\frac{IA}{g}\right] \sum_{l\geq 0} c_l^{(I)} g^l \, . \tag{2}$$

In this thesis, we have studied the trans-series and Resurgence structures of a well-known function in quantum field theory known as the "Euler-Heisenberg Lagrangian" (EHL). The EHL, first introduced by its namesakes Euler and Heisenberg in 1936 [10], describes non-linear corrections to the classical Maxwellian Lagrangian in the case of constant electromagnetic fields due to quantum fluctuations of particle fields. The fluctuating particle fields can be either spinor or scalar fields, in which case the underlying theory will be given by quantum electrodynamics (QED) and scalar quantum electrodynamics (sQED) respectively. In both of these cases, there is a well-known sector of instability in the case of a purely electric field background— a constant electric field in vacuum decays to give spontaneous production of particle anti-particle pairs in a process commonly known as Schwinger pair production [11]. Because of the instability in this sector, we can expect from Dyson's argument that the perturbative expansion of the EHL should be asymptotic. This has indeed proved to be the case in recent works on the subject of Resurgence of the EHL of QED [12,13]. However, the matter of Resurgence for the EHL of sQED was previously unstudied before our work on the subject [9].

The EHL can be arranged into different "loop orders", such that it is schematically given as

$$\mathscr{L}_{EH} = -\frac{1}{4}F^{\mu\nu}F_{\mu\nu} + \sum_{l=1}^{\infty}\mathscr{L}^{(l)} \,, \tag{3}$$

where the first term on the right hand side is the classical Maxwellian Lagrangian and $\mathscr{L}^{(l)}$ is the l^{th} loop correction to the EHL. Each loop correction is a function of the constant electromagnetic fields $B = |\mathbf{B}|$ and $E = |\mathbf{E}|$ in terms of the Lorentz invariant quantities $B^2 - E^2$ and $\mathbf{B}.\mathbf{E}$. While it is indeed possible to find an exact integral form of the EHL upto two loops, the task of computing an exact closed form becomes extremely difficult to compute. Instead, it is relatively simpler to perturbatively expand each loop contribution $\mathscr{L}^{(l)}$ in the weak field limit $E \to 0$ and $B \to 0$. In the case of a constant magnetic field background, this perturbative expansion can be found in terms of the dimensionless quantity qB/m^2 such that

$$\mathscr{L}^{(l)} \propto m^4 \alpha^{l-1} \sum_{n=0}^{\infty} a_n^{(l)} \left(\frac{qB}{m^2}\right)^{2n} \,, \; \frac{qB}{m^2} \to 0 \,, \tag{4}$$

where $\alpha = q^2/4\pi$. As we have shown in the later parts of the thesis, the coefficients of this perturbative expansion are factorially divergent and therefore is an asymptotic expansion that diverges in every domain. However, it is possible to "reconstruct" the underlying function by just using the asymptotic expansion above. The method that has been in recent for this sort of reconstruction is the "Padé-Borel resummation" [1], using which one can reconstruct the underlying function using only finite number of these perturbative terms and predict the non-perturbative behaviour of the function using this reconstruction upto remarkable accuracy.

The first loop correction $\mathscr{L}^{(1)}$ for QED was computed in the integral form by Euler and Heisenberg [10] and a similar form was subsequently calculated for the sQED EHL [14]. The integral form for the 2-loop EHL is much more involved to compute than its 1-loop counterpart and was first computed by Ritus for both QED and sQED [15, 16]. However, Ritus failed to recognize the non-triviality of the 1-PR contributions to the 2-loop EHL. The 1-PR diagrams of the 2-loop EHL were left unconsidered until very recently, when Gies and Karbstein proved that the 1-PR contributions are, in fact, non-zero, and can even dominate the 2-loop contributions to the EHL in the strong field limit [17]. In the literature, the trans-series structure has been studied for the 1-loop and 2-loop EHL for QED in the works of Florio and Dunne [12, 13]. However, similar studies have not been conducted for the sQED EHL before our work [9]. Additionally, these studies do not include any analysis of 1-PR diagrams.

In this thesis, we have reconstructed the EHL for the two cases— (i) $B=0$ or $E=0$ and (ii) $\mathbf{E} \parallel \mathbf{B}$. These two cases are inclusive of all the possible configurations of $\mathbf{E}$ and $\mathbf{B}$ upto a Lorentz transformation. We will call case (i) the "one-field" EHL and case (ii) the two-field EHL. For the one-field EHL, we have studied the resurgent properties for only the sQED EHL upto one and two loops, as similar studies have been for the QED EHL. Resurgence in the two-field EHL has not been studied in the literature as far as we are aware, and we have conducted this study for QED at the order of 1-loop. We have used the method of Padé-Borel resummation to reconstruct the EHLs using finite number of perturbative coefficients and have compared the reconstructed functions to either exact form of the function or its numerical estimates.

In Sec. 2.1, we calculate the unrenormalized form of the 1-loop and 2-loop EHL for sQED using the path integral formalism. In Sec. 2.2, we renormalize the integrals obtained in Sec.2.1 to get the final integral for the 1-loop and 2-loop EHL for sQED. In addition, we also find the closed forms for the 1-loop and the 2-loop 1-PR contributions to the EHL; the latter was not known before our work on the subject. In Sec. 2.3, we define the Padé-Borel sum in our convention. In Sec 3, we apply these Padé-Borel sums to the one-field EHL for sQED at one and two loops, and to the two-field EHL for QED at one loop.

2 Theoretical Methods and Calculations

This section is divided into three parts— Sec. 2.1 details how to find the EHL starting from the fundamental sQED Lagrangian, Sec. 2.2 details how the raw form of the EHL found in Sec. 2.1 is simplified and renormalized to find the integral form, and Sec. 2.3 explains how the integral form is used to find a Padé-Borel reconstructed form of the function.

2.1 Computing the sQED EHL

The EHL describes the Lagrangian of an "external" constant electromagnetic field produced by a source J. This source J, by definition, creates a electromagnetic field with the potential A. The distinction of the electromagnetic field being externally produced is essential to make in order to understand the formalism of the EHL. The details of the construction of the EHL are given in [17]. The EHL, after this construction, is given in the path integral form as

$$\Gamma_{\mathrm{HE}}[A] = \int d^4x \left(-\frac{1}{4}F_{\mu\nu}F^{\mu\nu}\right) + W[A]\,, \tag{5}$$

where the "vacuum persistence amplitude" $W[A]$ is given by

$$\exp(iW[A]) = \int \mathscr{D}\widetilde{A}\ \exp\left[i\int d^4x \left(-\frac{1}{4}\widetilde{F}^2_{\mu\nu} + \mathscr{L}_\phi[A+\widetilde{A}]\right)\right]\,. \tag{6}$$

$\widetilde{A}$ is the quantum fluctuation in the field A, and $\mathscr{L}_\phi$ is the scalar QED Lagrangian with the Maxwellian part omitted and the scalar field integrated out and is given as

$$\exp\left(i\mathscr{L}_\phi[A]\right) = \int \mathscr{D}\phi\mathscr{D}\phi^*\exp\left(i\mathscr{L}[\phi,A]\right)\,, \tag{7}$$

where $\mathscr{L}[\phi,A]$ is given by

$$\begin{aligned}\mathscr{L}[\phi,A] &= (D_\mu\phi)^*(D^\mu\phi) - m^2\phi^*\phi \\ &= (\partial_\mu\phi^*)(\partial^\mu\phi) + iq[(\partial_\mu\phi^*)(A^\mu\phi) - (\partial_\mu\phi)(A^\mu\phi^*)] + q^2A^2\phi^*\phi - m^2\phi^*\phi\,.\end{aligned} \tag{8}$$

A_μ is the electromagnetic four potential, ϕ is the scalar field, $F_{\mu\nu} = \partial_\mu A_\nu - \partial_\nu A_\mu$ is the electromagnetic tensor, and $D_\mu = \partial_\mu + iqA_\mu$ is the covariant derivative. It can be shown that eq. (6) can be rewritten as [18]

$$\exp(iW[A]) = \exp\left(\frac{1}{2}\frac{\delta}{\delta J}D_+\frac{\delta}{\delta J}\right)\exp\left(i\overline{W}^{(1)}[A+J]\right)\Big|_{J=0}\,, \tag{9}$$

$\overline{W}^{(1)}$ being the Wilsonian action defined as

$$\overline{W}^{(1)}[A] = \int d^4x\, \mathscr{L}_\phi[A]\,, \tag{10}$$

$D_+^{\mu\nu}(x-y) = g^{\mu\nu}D_+(x-y)$ is the photon propagator, and the operator shorthand is defined as

$$\frac{\delta}{\delta J}D_+\frac{\delta}{\delta J} = \int d^4x d^4y \, \frac{\delta}{\delta J(y)}D_+(x-y)\frac{\delta}{\delta J(x)} \, . \tag{11}$$

The operator in the right hand side of eq. (9) can be written as an expansion of an exponential. Each successive term of this expansion will be an order of α higher than the previous term. The l^{th} term in this expansion is known as the l-loop correction of the EHL.

In the following subsections, we will simplify eq. (9) to find the raw forms of the 1-loop and 2-loop EHLs, which we will further simplify to give integral forms in Sec. 2.2.

2.1.1 1-loop sQED EHL

The 1st term of the expansion in eq. (9) is easily seen to be

$$W^{(1)}[A] = \overline{W}^{(1)}[A] \, . \tag{12}$$

To compute $\overline{W}^{(1)}$, we will differentiate both sides of eq. (7) with respect to A_μ to get that

$$\frac{\partial \mathscr{L}_\phi}{\partial A_\mu}(x) = -iq \langle A| \phi^*(x)(D^\mu\phi(x)) - \phi(x)(D^\mu\phi(x))^* |A\rangle \, , \tag{13}$$

where $|A\rangle$ in the expectation value denotes that the expectation value is computed in the presence of the external field A. To simplify the right hand side, we will write it as a limit such that

$$\frac{\partial \mathscr{L}_\phi}{\partial A_\mu}(x) = -iq \lim_{\Delta x\to 0} \frac{\langle A| \phi^*(x)\phi(x+\Delta x) - \phi(x)\phi^*(x+\Delta x) |A\rangle}{\Delta x} \\ + 2q^2 A^\mu \langle A| \phi^*(x)\phi(x) |A\rangle \, . \tag{14}$$

Now, using translational invariance of the second term to shift $x \to x - \Delta x$ to get that

$$\frac{\partial \mathscr{L}_\phi}{\partial A_\mu} = -2iq \lim_{y\to x} D_x^\mu G_A(x-y) \, , \tag{15}$$

where $G_A(x-y)$ is the scalar field Green's function in the background electromagnetic field. This Green's function, in the Schwinger proper time formalism, may be expressed as [19]

$$G_A(x-y) = \langle A| \widehat{T}\left[\phi(x)\phi^*(y)\right] |A\rangle = \int_0^\infty ds \, e^{-s\epsilon} e^{-ism^2} \langle x| e^{-i\widehat{H}s} |y\rangle \, . \tag{16}$$

$\widehat{T}$ denotes time ordering, and $\widehat{H} = -(\widehat{p} - q\widehat{A})^2$, where $\widehat{p}^\mu$ is the momentum operator, and $\widehat{A}^\mu = A^\mu(\widehat{x})$.

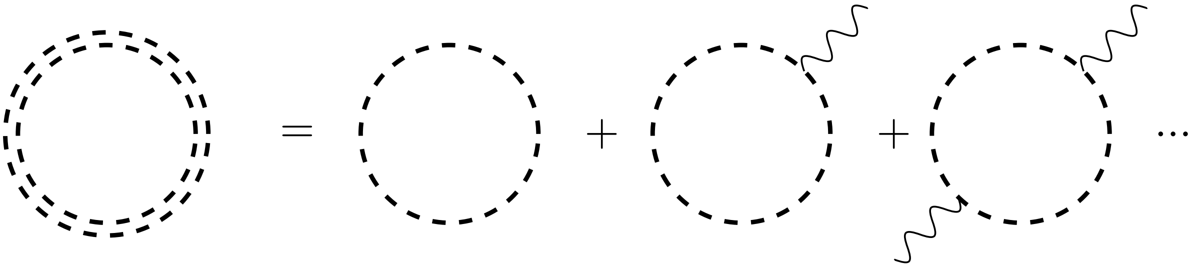

Figure 1: Diagrammatic representation of the 1-loop EHL of sQED using "dressed propagators". A dressed propagator, depicted as a double line, is given as an infinite sum of a combination of scalar propagators appended by variable number of external electromagnetic field legs.

Operating both sides of eq. (16) by D^μ_x gives rise to a total partial derivative on the right-hand side such that

$$D^\mu_x G_A(x-y) = \frac{1}{2q}\frac{\partial}{\partial A_\mu}\int_0^\infty \frac{ds}{s}\, e^{-s\epsilon} e^{-ism^2}\,\langle x|\, e^{-i\widehat{H}s}\,|x\rangle\ . \tag{17}$$

Substituting this in eq. (15) gives us the result for the 1-loop Lagrangian in Schwinger proper time–

$$\boxed{\mathscr{L}_\phi(x) = -i\int_0^\infty \frac{ds}{s}\, e^{-s\epsilon} e^{-ism^2}\,\langle x|\, e^{-i\widehat{H}s}\,|x\rangle}\ . \tag{18}$$

This integral has a popular and suggestive diagrammatic representation in fig. 1.

2.1.2 2-loop sQED EHL

Upto the second order, the expansion of eq. (9) is given by

$$1 + iW^{(1)}[A] + iW^{(2)}[A] + \ldots =$$
$$\left[1 + \frac{1}{2}\frac{\delta}{\delta J}D_+\frac{\delta}{\delta J}\right]\left[1 + i\overline{W}^{(1)}[A] + iJ\frac{\delta\overline{W}^{(1)}[A]}{\delta A} + \frac{iJ^2}{2}\frac{\delta^2\overline{W}^{(1)}[A]}{\delta A^2} - \frac{J^2}{2}\left(\frac{\delta\overline{W}^{(1)}[A]}{\delta A}\right)^2\right]\Bigg|_{J=0} + \mathscr{O}(\alpha^2)\,. \tag{19}$$

Therefore, $W^{(2)}[A]$ is seen to have two terms— the 1-PI and 1-PR terms given by

$$W^{(2)}_{\text{1-PI}}[A] = \frac{1}{2}\int d^4x d^4y\, \frac{\delta^2\overline{W}^{(1)}}{\delta A^\mu(y)\delta A^\nu(x)} D^{\mu\nu}_+(x-y)\,, \tag{20}$$

and

$$W^{(2)}_{\text{1-PR}}[A] = \frac{i}{2}\int d^4x d^4y\, \frac{\delta\overline{W}^{(1)}}{\delta A^\mu(x)}\frac{\delta\overline{W}^{(1)}}{\delta A^\nu(y)} D^{\mu\nu}_+(x-y)\ . \tag{21}$$

The diagrammatic representations of each of these terms are given in fig. 2.

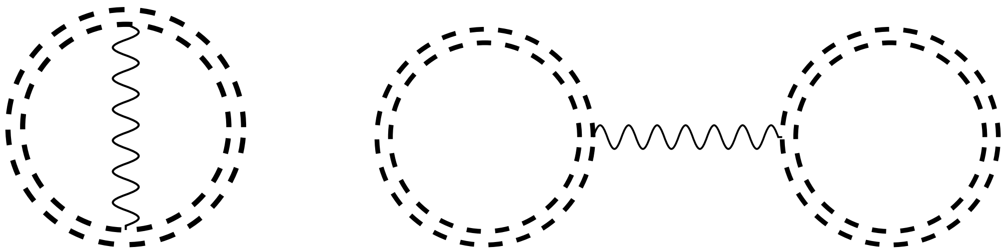

(a) (b)

Figure 2: Diagrammatic representation of the 2-looop EHL of sQED. The 2-loop EHL contains two parts— the 1-PI part depicted in fig. 2a and the 1-PR part depicted in fig. 2b.

We will first calculate a more tractable expression for the 1-PI contribution to the 2-loop EHL. A simplified expression for the 1-PR contribution is much more subtle to calculate and has been calculated in [17].

1-PI diagram

The approach towards calculating the 2-loop 1-PI EHL has been adopted from [18]. To simplify eq. (20), we will first have to find the second functional derivative of $\overline{W}^{(1)}$. From eq. (15), we already know that the first functional derivative is related to the Green's function of the scalar field. We also know that the Green's function satisfies the field equation

$$(D_z^2 + m^2)G_A(z-y) = -i\delta^4(z-y) \,. \tag{22}$$

Now, we multiply by the free scalar propagator $G_F(x-z)$ on both sides and integrate over the z space, expand the covariant derivative, and use the identity

$$G_F(x-z)\partial_z^2 G_A(z-y) = G_A(z-y)\partial_z^2 G_F(x-z) - \partial_z(G_A(z-y)\partial_z G_F(x-z)) + \\ \partial_z(G_F(x-z)\partial_z G_A(z-y)) \,, \tag{23}$$

to get the relation

$$-iG_A(x-y) - q^2\int d^4z\, A^2(z)G_A(z-y)G_F(x-z) + 2iq\int d^4z\, A(z)G_F(x-z)\partial_z G_A(z-y) + \\ iq\int d^4z\, \partial A(z)G_F(x-z)G_A(z-y) = -iG^F(x-y) \,. \tag{24}$$

This equation, in the operator notation, can be written as

$$\widehat{G}_A = \widehat{G}_F + iq^2\widehat{G}_F\widehat{A}^2\widehat{G}_A - 2iq\widehat{G}_F\widehat{A}\widehat{p}\widehat{G}_A + q\widehat{G}_F\partial\widehat{A}\widehat{G}_A \,, \tag{25}$$

where $\widehat{p}^\mu$ is the momentum operator, $\widehat{A}^\mu = A^\mu(\widehat{x})$, the operator $\widehat{G}_A$ is defined as $\langle x|\widehat{G}_A|y\rangle = G_A(x-y)$, and $\widehat{G}_F$ is defined in a similar manner. It will be useful to keep in mind that this equation can be rearranged to give

$$\widehat{G}_A = (1 - iq^2\widehat{G}_F\widehat{A}^2 + 2iq\widehat{G}_F\widehat{A}\widehat{p} - q\widehat{G}_F\partial\widehat{A})^{-1}\widehat{G}_F\ . \tag{26}$$

Now, we will take a functional derivative on both sides of eq. (24) to get that

$$\begin{aligned}
&\frac{\delta G_A(x-y)}{\delta A_\mu(w)} = \\
&\quad iq^2\int d^4z\left[2G_F(x-z)A^\mu(z)\delta^4(z-w)G_A(z-y) + G_F(x-z)A^2(z)\frac{\delta G_A(z-y)}{\delta A_\mu(w)}\right] \\
&\quad + 2q\int d^4z\left[G_F(x-z)\delta^4(z-w)\partial_z G_A(z-y) + G_F(x-z)A(z)\partial_z\frac{\delta G_A(z-y)}{\delta A_\mu(w)}\right] \\
&\quad + q\int d^4z\left[G_F(x-z)\partial_z^\mu(\delta^4(z-w))G_A(z-y) + G_F(x-z)\partial A(z)\frac{\delta G_A(z-y)}{\delta A_\mu(w)}\right]\ .
\end{aligned} \tag{27}$$

A couple of simplifications can be done to arrive at the final answer–

$$\partial_z^\mu(\delta^4(z-w))G_A(x-z)G_A(z-y) = -\delta^4(z-w)\partial_z^\mu(G_A(x-z)G_A(z-y))\ , \tag{28}$$

and

$$\begin{aligned}
\partial_z^\mu\langle x|\widehat{G}_A|z\rangle &= (\partial_z^\mu\langle z|\widehat{G}_A^\dagger|x\rangle)^*\ , \\
&= (-i\langle z|\widehat{p}^\mu\widehat{G}_A^\dagger|x\rangle)^*\ , \\
&= i\langle x|\widehat{G}_A\widehat{p}^\mu|z\rangle\ .
\end{aligned} \tag{29}$$

After this simplification, we will use eq. (26) to arrive at the first functional derivative of G_A,

$$\frac{\delta\widehat{G}_A}{\delta A_\mu(w)} = -iq\left[\left(\widehat{G}_A|w\rangle\langle w|\widehat{\Pi}^\mu\widehat{G}_A\right) + \left(\widehat{G}_A\widehat{\Pi}^\mu|w\rangle\langle w|\widehat{G}_A\right)\right]\ , \tag{30}$$

where $\widehat{\Pi}^\mu = \widehat{p}^\mu - \widehat{A}^\mu$. Substituting this in eq. (20), we have that

$$\boxed{\begin{aligned}
W^{(2)}_{\text{1-PI}}[A] = -iq^2\int d^4x d^4y\Big[&4i\delta^4(x-y)\langle x|\widehat{G}_A|y\rangle - \langle x|\widehat{\Pi}^\mu\widehat{G}_A|y\rangle\langle y|\widehat{\Pi}_\mu\widehat{G}_A|x\rangle - \\
&\langle x|\widehat{\Pi}^\mu\widehat{G}_A\widehat{\Pi}_\mu|y\rangle\langle y|\widehat{G}_A|x\rangle\Big]D_+(x-y)\ .
\end{aligned}} \tag{31}$$

1-PR diagram

The non-triviality of eq. (21) was proved very recently [17]. The proof relies on the delicate cancellations between divergences in the photon propagator D_+ and the vanishing tendency of the propagator G_A in the limit of a constant electromagnetic field. It is shown in the same work that the 1-PR contribution is given by

$$\boxed{W^{(2)}_{\text{1-PR}}[A] = \frac{1}{2}\int d^4x\, \frac{\partial \mathscr{L}^{(1)}}{\partial F^{\mu\nu}}\frac{\partial \mathscr{L}^{(1)}}{\partial F_{\mu\nu}}\,.} \tag{32}$$

In the following subsection, we will simplify the boxed expressions in eq. (18), (31) and (32) and renormalize to give the integral forms for these EHL contributions.

2.2 Renormalization of sQED EHL

In our analysis, we will see that the expressions for the 1-loop and 2-loop EHLs in eq. (18), (31) and (32) are actually divergent. However, all these expressions can be renormalized to give a finite answer. In the following subsections, we will renormalize all the three expressions in eq. (18), (31) and (32).

2.2.1 1-loop sQED EHL

To simplify eq. (18), we will need an expression for $\langle x|\, e^{-i\widehat{H}s}\,|x\rangle$. This was found by Schwinger [11] and is given by

$$\langle x|\, e^{-i\widehat{H}s}\,|x\rangle = -\frac{i}{16\pi^2}\frac{e^{-L(s)}}{s^2}\,, \tag{33}$$

where $L(s)$ is given by

$$L(s) = \frac{1}{2}\mathrm{Tr}\log[(qFs)^{-1}\sinh(qFs)]\,. \tag{34}$$

Now, notice that $e^{-L(s)}$ can be simplified as

$$\begin{aligned}\exp\left[-\frac{1}{2}\mathrm{tr}\log\left(\frac{\sinh(qFs)}{qFs}\right)\right] &= \det\left[\exp\left(-\frac{1}{2}\log\left(\frac{\sinh(qFs)}{qFs}\right)\right)\right] \\ &= \det\left[\frac{qFs}{\sinh(qFs)}\right]^{1/2} \\ &= \frac{q^2s^2\eta\epsilon}{\sin(q\eta s)\sinh(q\epsilon s)}\,,\end{aligned} \tag{35}$$

where $i\eta$ and ϵ are the two eigenvalues of the electromagnetic matrix F and are given by

$$\epsilon = \sqrt{\sqrt{\mathscr{F}^2+\mathscr{G}^2}-\mathscr{F}} \tag{36a}$$

$$\eta = \sqrt{\sqrt{\mathscr{F}^2+\mathscr{G}^2}+\mathscr{F}}\,, \tag{36b}$$

where $\mathscr{F}$ and $\mathscr{G}$ are given by

$$\mathscr{F} = \frac{1}{4} F^{\mu\nu} F_{\mu\nu} \tag{37a}$$

$$\mathscr{G} = \frac{1}{4} F^{\mu\nu} \widetilde{F}_{\mu\nu} \ . \tag{37b}$$

($\widetilde{F}$ is the electromagnetic dual tensor). Therefore, $\mathscr{L}^{(1)}$ is given by

$$\mathscr{L}^{(1)} = -\frac{1}{16\pi^2} \int_0^\infty \frac{ds}{s^3}\, e^{-s\varepsilon} e^{-ism^2}\, \frac{q^2 s^2 \eta \epsilon}{\sin(q\eta s)\sinh(q\epsilon s)} \ . \tag{38}$$

Notice that as $\eta, \epsilon \to 0$, $\mathscr{L}^{(1)}$ diverges. However, notice that in this limit, the integrand can be expanded as

$$\frac{q^2 s^2 \eta \epsilon}{\sin(q\eta s)\sinh(q\epsilon s)} = 1 - \frac{q^2(\epsilon^2 - \eta^2)s^2}{6} + \text{higher order terms} \ , \ \eta, \epsilon \to 0 \ . \tag{39}$$

Both of the terms of this expansion can be renormalized into the vacuum energy and the Maxwellian parts. Subtracting these terms from the integrand gives us a finite answer—

$$\mathscr{L}^{(1)} = -\frac{1}{16\pi^2} \int_0^\infty \frac{ds}{s^3}\, e^{-s\varepsilon} e^{-ism^2} \left[\frac{q^2 s^2 \eta \epsilon}{\sin(q\eta s)\sinh(q\epsilon s)} - 1 + \frac{q^2(\epsilon^2 - \eta^2)s^2}{6} \right] \ . \tag{40}$$

It is now customary to perform the contour rotation $s \to -is$ to get that

$$\boxed{\mathscr{L}^{(1)} = \frac{1}{16\pi^2} \int_0^\infty \frac{ds}{s^3}\, e^{-sm^2} \left[\frac{q^2 s^2 \eta \epsilon}{\sinh(q\eta s)\sin(q\epsilon s)} - 1 + \frac{q^2(\eta^2 - \epsilon^2)s^2}{6} \right]} \ . \tag{41}$$

In the limit $\epsilon \to 0$, this integral is given by

$$\mathscr{L}^{(1)} = \frac{q^2 B^2}{16\pi^2} \int_0^\infty \frac{ds}{s^2} e^{-sm^2/qB} \left[\frac{1}{\sinh s} - \frac{1}{s} + \frac{s}{6} \right] \tag{42}$$

We can find a closed form for this integral. To do this, we will use the identities

$$\int_0^\infty ds\, s^{\nu-1} e^{-\beta s} = \beta^{-\nu}\, \Gamma(\nu) \ , \tag{43a}$$

$$\int_0^\infty ds\, s^{\nu-1} \frac{1}{\sinh s}\, e^{-\beta s} = 2^{1-\nu}\, \Gamma(\nu)\, \zeta_H\left(\nu, \frac{1+\beta}{2}\right) \ , \tag{43b}$$

where ζ_H is the Hurwitz-Zeta function. These identities are only valid for Re $\beta > 0$ and Re $\nu > 0$, and hence cannot be applied to eq. (137) directly. To perform an appropriate analytic continuation, we introduce the parameter ϵ in the integral–

$$\lim_{\epsilon \to 0} \int_0^\infty \frac{ds}{s^{2-\epsilon}}\, e^{-m^2 s/qB} \left[\frac{1}{\sinh s} - \frac{1}{s} + \frac{s}{6} \right] \ . \tag{44}$$

The individual integrals in eq. (44) can now be performed and, in the leading and first subleading order, be written as

$$\int_0^\infty \frac{ds}{s^{2-\epsilon}}\,\frac{1}{\sinh s}\,e^{-m^2 s/qB} = -\frac{4}{\epsilon}\,\zeta_H\left(-1,\frac{1+m^2/qB}{2}\right)+\zeta_H\left(-1,\frac{1+m^2/qB}{2}\right)(4\log 2-4+4\gamma)- 4\zeta_H'\left(-1,\frac{1+m^2/qB}{2}\right)\,, \tag{45}$$

where the derivative of the Hurwitz-zeta function is with respect to the first argument and

$$\int_0^\infty \frac{ds}{s^{3-\epsilon}}\,e^{-m^2 s/qB} = \frac{1}{2}\left(\frac{m^2}{qB}\right)^2\left[\frac{1}{\epsilon}+\frac{3}{2}-\gamma-\log\left(\frac{m^2}{qB}\right)\right]\,, \tag{46a}$$

$$\int_0^\infty \frac{ds}{s^{1-\epsilon}}\,e^{-m^2 s/qB} = \frac{1}{\epsilon}-\log\left(\frac{m^2}{qB}\right)-\gamma\,. \tag{46b}$$

Using the property of the zeta function,

$$\zeta_H\left(-1,\frac{1+x}{2}\right) = \frac{1}{24}-\frac{x^2}{8}\,, \tag{47}$$

we see that the divergent parts in the integral cancel out, and the finite part that remains is

$$\mathscr{L}^{(1)} = -\frac{m^4}{16\pi^2}\left(\frac{2qB}{m^2}\right)^2\left[\zeta_H'\left(-1,\frac{1}{2}+\frac{m^2}{2qB}\right)+\frac{3}{4}\left(\frac{m^2}{2qB}\right)^2+ \left(1+\log\left(\frac{m^2}{2qB}\right)\right)\zeta_H\left(-1,\frac{1}{2}+\frac{m^2}{2qB}\right)\right]\,. \tag{48}$$

2.2.2 2-loop 1-PI diagram

To simplify eq. (31), we need an expression for G_A and D_+. This expression is also given in the proper time formalism by Schwinger [11]–

$$D_+(x-y) = \frac{i}{16\pi^2}\int_0^\infty \frac{ds}{s^2}\,\exp\left[\frac{-i(x-y)^2}{4s}-\varepsilon s\right]\,, \tag{49}$$

and

$$G_A(x-y) = -\frac{i}{16\pi^2}\Phi(x,y)\int_0^\infty \frac{ds}{s^2}\,e^{-s\varepsilon}\exp\left[-\frac{i}{4}z^\mu\beta_{\mu\nu}(s)z^\nu-L(s)-ism^2\right]\,, \tag{50}$$

where $\Phi(x,y)$ is the gauge-dependent phase the final answer is independent of, $z=x-y$, and the matrix β is given by

$$\beta = qF\coth(qFs)\,. \tag{51}$$

Now, we can easily compute that

$$\begin{aligned}\langle x|\,\widehat{\Pi}^\mu G_A\,|y\rangle &= (i\partial_\mu-qA_\mu)G_A(x-y)\,,\\ &= -\frac{i}{16\pi^2}\Phi(x,y)\int_0^\infty \frac{ds}{s^2}\,e^{-s\varepsilon}\frac{1}{2}\Big(qF^{\mu\nu}z_\mu+\beta^{\mu\nu}(s)z_\nu\Big)\exp\left[-\frac{i}{4}z\beta(s)z-L(s)-ism^2\right]\,,\end{aligned} \tag{52}$$

$$\begin{aligned}\langle x|\,G_A\widehat{\Pi}^\mu\,|y\rangle &= \Big(\langle y|\,\widehat{\Pi}_\mu(\widehat{G}_A)^*\,|x\rangle\Big)^*\,,\\ &= -\frac{i}{16\pi^2}\Phi(x,y)\int_0^\infty\frac{ds}{s^2}\,e^{-s\varepsilon}\frac{1}{2}\Big(-qFz+\beta(s)z\Big)\exp\left[-\frac{i}{4}z\beta(s)z-L(s)-ism^2\right]\,.\end{aligned} \tag{53}$$

To find $\langle x|\,\widehat{\Pi}^\mu G_A\widehat{\Pi}_\mu\,|y\rangle$, we can use a relation that is apparent from eqs. (52) and (53):

$$\widehat{G}_A\widehat{\Pi}_\mu = \widehat{\Pi}_\mu\widehat{G}_A - qFz\widehat{G}_A\,. \tag{54}$$

Multiplying both sides by $\widehat{\Pi}^\mu$, taking an expectation value, and using Green's equation for the evolution of G_A, we have the simplified relation

$$\langle x|\,\widehat{\Pi}^\mu\widehat{G}_A\widehat{\Pi}_\mu\,|y\rangle = i\delta^4(x-y)+m^2G_A(x-y)-\frac{q^2}{2}(zFFz)G_A(x-y)\,. \tag{55}$$

Notice that each term of the integrand is only dependent on $z=x-y$. Therefore, we can perform a variable change in eq. (31) to get that

$$\int d^4y\mathscr{L}^{(2)}_{\text{1-PI}} = -iq^2\int d^4z\,d^4y\ \text{Integrand(z)}\,, \tag{56}$$

which gives us that

$$\mathscr{L}^{(2)}_{\text{1-PI}} = -iq^2\int d^4z\ \text{Integrand(z)}\,. \tag{57}$$

Now, we will tackle each term of the integrand separately.

Delta term

We'll start with the easy term, which is

$$H_1 = -\frac{i}{16\pi^2}\int_0^\infty\frac{ds}{s^2}e^{-s\epsilon}\int d^4z\,3i\,D_+(z)\delta^4(z)\exp\left[-L(s)-ism^2\right]\,. \tag{58}$$

Using the proper time form of D_+ in eq. (49) and the value of $e^{-L(s)}$ we derived in Sec. 2.2.1, we get that

$$H_1 = \frac{3i}{(4\pi)^2}\int_0^\infty\frac{ds}{s^2}\int_0^\infty\frac{dt}{t^2}\,\frac{q^2s^2\eta\epsilon}{\sinh(q\eta s)\sin(q\epsilon s)}e^{-ism^2}\,. \tag{59}$$

Notice that the t integral is divergent. To regularize it, we introduce a lower bound t_0 and perform the integral. Doing this, we get that

$$H_1 = \frac{3iq^2}{(4\pi)^4t_0}\int_0^\infty ds\,\frac{\eta\epsilon}{\sin(q\eta s)\sinh(q\epsilon)}e^{-ism^2}\,. \tag{60}$$

Notice that this integral looks very similar to the unrenormalized one-loop Lagrangian correction. More precisely,

$$H_1 = \frac{3}{16m^2\pi^2t_0}\frac{\partial\mathscr{L}^{(1)}_{\text{UR}}}{\partial m^2}\,. \tag{61}$$

In terms of the renormalized one-loop Lagrangian, this is written as

$$H_1 = \frac{3}{16m^2\pi^2 t_0}\frac{\partial \mathscr{L}_{\mathrm{R}}^{(1)}}{\partial m^2} + \frac{3U_1}{16\pi^2 t_0} - \frac{q^2 U_2}{32\pi^2 m^2 t_0}\,, \tag{62}$$

where U_1 and U_2 are the divergent integrals

$$U_1 = \int_0^\infty \frac{ds}{s^2} e^{-im^2 s}\,, \tag{63a}$$

$$U_2 = \int_0^\infty ds\, e^{-ism^2}\,. \tag{63b}$$

Therefore, we must renormalize the ground energy and the free Lagrangian to a different value after the addition of the second-loop correction. Also, the partial derivative term is exactly the mass correction to the effective Lagrangian.

Gaussian term

We get one term of the form

$$-m^2 \int d^4z\, G^A(z) D(z) G^A(-z)\,. \tag{64}$$

Expanding the integral in proper time coordinates, we get

$$H_2 = \frac{im^2}{(4\pi)^6}\int d^4z \int \frac{ds}{s^2}\int \frac{ds'}{(s')^2}\int \frac{dt}{t^2} e^{-(s+s')\epsilon} e^{-i(s+s')m^2} \exp\left[-\frac{i}{4} z(\beta+\beta')z - L - L'\right] \exp\left[-\frac{iz^2}{4t}\right]\,. \tag{65}$$

We will do the spacetime integration first. It is a simple Gaussian integration which gives us

$$\frac{im^2}{(4\pi)^6}\int \frac{ds}{s^2}\int \frac{ds'}{(s')^2}\int \frac{dt}{t^2} e^{-(s+s')\epsilon} e^{-i(s+s')m^2} e^{-L-L'} \left(\frac{(4\pi i)^4}{\det \mathscr{M}}\right)^{1/2}\,, \tag{66}$$

where $\mathscr{M}$ is the operator

$$\mathscr{M} = \beta + \beta' + \frac{1}{t}\,. \tag{67}$$

Since β and β' are simultaneously diagonalizable, the determinant is given by

$$[\det \mathscr{M}]^{1/2} = \left(q\eta\cot(q\eta s) + q\eta\cot\big(q\eta s'\big) + \frac{1}{t}\right)\left(q\epsilon\coth(q\epsilon s) + q\epsilon\coth\big(q\epsilon s'\big) + \frac{1}{t}\right)\,. \tag{68}$$

Calling

$$a = q\eta\cot(q\eta s) + q\eta\cot\big(q\eta s'\big) \tag{69a}$$

$$b = q\epsilon\coth(q\epsilon s) + q\epsilon\coth\big(q\epsilon s'\big)\,, \tag{69b}$$

we finally get

$$H_2 = -\frac{im^2}{(4\pi)^4}\int \frac{ds}{s^2}\int \frac{ds'}{(s')^2}\int \frac{dt}{t^2} e^{-(s+s')\epsilon} e^{-i(s+s')m^2} e^{-L-L'} \left(\frac{1}{a+\frac{1}{t}}\cdot\frac{1}{b+\frac{1}{t}}\right) . \tag{70}$$

Doing the t integration then gives us

$$H_2 = -\frac{im^2}{(4\pi)^4}\int ds \int ds'\; e^{-(s+s')\epsilon} e^{-i(s+s')m^2}$$
$$\frac{q^4\eta^2\epsilon^2}{\sin(q\eta s)\sin(q\eta s')\sinh(q\epsilon s)\sinh(q\epsilon s')}\frac{1}{b-a}\log\left(\frac{b}{a}\right) . \tag{71}$$

Calling

$$P = \sin(q\eta s)\sinh(q\epsilon s) \tag{72a}$$

$$J_0 = \frac{1}{b-a}\log\left(\frac{b}{a}\right) , \tag{72b}$$

we have (including the q^2 factor in the Lagrangian)

$$H_2 = -\frac{iq^6m^2}{256\pi^4}\int_0^\infty ds \int_0^\infty ds'\; e^{-i(s+s')(m^2-i\epsilon)}\frac{\eta^2\epsilon^2}{PP'}J_0 . \tag{73}$$

Quadratic Gaussian term

The third type of term is the term

$$H_3 = \int d^4z\;\left(\frac{3q^2}{4}zFFz + \frac{1}{4}z\beta\beta z\right) G^A(z)D(z)G^A(-z) . \tag{74}$$

Expanding this gives us

$$-\frac{i}{(4\pi)^6}\int d^4z \int ds \int ds' \int \frac{dt}{t^2}\; e^{-i(s+s')(m^2-i\epsilon)}\frac{\eta^2\epsilon^2}{PP'}$$
$$\left(\frac{3q^2}{4}zFFz + \frac{1}{4}z\beta\beta z\right)\exp\left[-\frac{i}{4}z\mathscr{M}z\right] . \tag{75}$$

These integrals are done by changing the variables to the diagonal basis and integrating over z. For example, the integral

$$\int d^4z\; (zFFz)\exp\left[-\frac{i}{4}z\mathscr{M}z\right] , \tag{76}$$

after integration is given by

$$4i\left[\frac{(i\eta)^2}{a+\frac{1}{t}} + \frac{\epsilon^2}{b+\frac{1}{t}}\right]\left(\frac{(4\pi i)^4}{\det\mathscr{M}}\right)^{1/2} . \tag{77}$$

After integration with t, this gives

$$\frac{(\epsilon^2+\eta^2)\log(b/a)}{(b-a)^2} - \frac{\frac{\epsilon^2}{b}+\frac{\eta^2}{a}}{(b-a)} \ . \tag{78}$$

Similarly, the other term after integrated over z gives

$$-4i\left[\frac{(q\eta)^2\cot(q\eta s)\cot(q\eta s')}{a+\frac{1}{t}} + \frac{(q\epsilon)^2\cot(q\epsilon s)\cot(q\epsilon s')}{b+\frac{1}{t}}\right]\left(\frac{(4\pi i)^4}{\det\mathscr{M}}\right)^{1/2} \ . \tag{79}$$

Define the quantities

$$p = 2(q\eta)^2(\cot(q\eta s)\cot\big(q\eta s'\big)+3) \tag{80a}$$

$$q = 2(q\epsilon)^2(\coth(q\epsilon s)\coth\big(q\epsilon s'\big)-3) \ , \tag{80b}$$

In terms of p and q, the final of the term is

$$H_3 = \frac{iq^4}{256\pi^4}\int_0^\infty ds\int_0^\infty ds'\ e^{-i(s+s')(m^2-i\epsilon)}\frac{\eta^2\epsilon^2}{PP'}\left(-\frac{i}{2}I\right) \ , \tag{81}$$

where J is given by

$$J = \frac{(q-p)\log(b/a)}{(b-a)^2} - \frac{\frac{q}{b}-\frac{p}{a}}{b-a} \ . \tag{82}$$

Adding all the terms, we get that [15]

$$\mathscr{L}^{(2)} = \frac{iq^2}{256\pi^4}\int_0^\infty ds\int_0^\infty ds'\ \frac{(q\eta)^2(q\epsilon)^2e^{-i(s+s')(m^2-i\epsilon)}}{\sin(q\eta s)\sin(q\eta s')\sinh(q\epsilon s)\sinh(q\epsilon s')}\left(m^2J_0+\frac{iJ}{2}\right) \ . \tag{83}$$

This is the unrenormalized Lagrangian with still a lot of divergences. We will now renormalize this Lagrangian.

Renormalization

As in the one-loop case, the divergences in the integral are due to the vacuum energy and a term that is proportional to the free Lagrangian. To find out these divergences we expand the integrand in powers of η and ϵ. We'll do this term by term:

1. The prefactor:

$$\mathrm{PF} = \frac{(q\eta)^2(q\epsilon)^2}{\sin(q\eta s)\sin(q\eta s')\sinh(q\epsilon s)\sinh(q\epsilon s')} \tag{84}$$

has the weak field expansion

$$\mathrm{PF} = \frac{1}{s^2s'^2}\left(1-\frac{q^2}{6}(\epsilon^2-\eta^2)(s^2+s'^2)\right) \ . \tag{85}$$

2. $\underline{J_0}$:

$$J_0 = \frac{1}{b-a} \log\left(\frac{b}{a}\right) \tag{86}$$

has the weak field expansion

$$J_0 = \frac{ss'}{s+s'}\left(1 - \frac{q^2}{6}(\epsilon^2 - \eta^2)ss'\right) . \tag{87}$$

3. $\underline{J}$:

$$J = \frac{(q-p)\log(b/a)}{(b-a)^2} - \frac{\frac{q}{b} - \frac{p}{a}}{b-a} \tag{88}$$

has the weak field expansion

$$J = \frac{2ss'}{(s+s')^2}\left(1 + \frac{q^2}{6}(\epsilon^2 - \eta^2)(s^2 - 11ss' + s'^2)\right) . \tag{89}$$

Therefore, the weak field expansion of the integrand F is given as

$$F(s,s') = \frac{1}{ss'(s+s')}\left[m^2\left(1 - \frac{q^2}{6}(\epsilon^2 - \eta^2)(s^2 + s'^2 + ss')\right)\right.$$
$$\left. + \frac{i}{s+s'}\left(1 - \frac{11q^2}{6}(\epsilon^2 - \eta^2)ss'\right)\right] . \tag{90}$$

These terms are all divergent, but we can subtract them from our Lagrangian because they are responsible for the renormalization of the theory. We denote the integrand that results after subtracting these divergences as $K(s,s')$. The integral of $K(s,s')$ is still not convergent because of the logarithmically divergent term due to the quadratic expansion term of I. We extract this term by finding the limit of $K(s,s')$ as $s' \to 0$ (or equivalently, $s \to 0$):

1. Prefactor:

$$\lim_{s' \to 0} \mathrm{PF} = \frac{1}{s'^2} \frac{(q\eta)(q\epsilon)}{\sin(q\eta s)\sinh(q\epsilon s)} \tag{91}$$

2. $\underline{J_0}$:

$$\lim_{s' \to 0} J_0 = s' \tag{92}$$

3. $\underline{J}$:

$$\lim_{s' \to 0} J = s'\Big(q\eta\ \cot(q\eta s) + q\epsilon\ \coth(q\epsilon s)\Big) \tag{93}$$

4. Divergent term:

$$\lim_{s' \to 0} \mathrm{div} = \frac{1}{s^2 s'}\left(m^2 - \frac{qm^2}{6}(\epsilon^2 - \eta^2)s^2 + \frac{i}{s}\right) \tag{94}$$

Therefore, we see that we can write $K(s,s')$ in the limit $s' \to 0$ as

$$\lim_{s'\to 0} K(s,s') = \frac{K_0(s)}{s'} \;, \tag{95}$$

where

$$K_0(s) = \frac{(q\eta)(q\epsilon)}{\sin(q\eta s)\sinh(q\epsilon s)}\left(m^2 + \frac{i}{2}\left(q\eta\ \cot(q\eta s) + q\epsilon\ \coth(q\epsilon s)\right)\right) - \frac{1}{s^2}\left(m^2 - \frac{qm^2}{6}(\epsilon^2-\eta^2)s^2 + \frac{i}{s}\right) \;. \tag{96}$$

Notice that this is exactly equal to

$$K_0(s) = \left(m^2 - \frac{i}{2}\frac{\partial}{\partial s}\right)\mathscr{L} \;, \tag{97}$$

where $\mathscr{L}$, upto a multiplicative factor, is the integrand in the proper time representation of the one-loop effective Lagrangian–

$$\mathscr{L}(s) = \frac{(q\epsilon)(q\eta)}{\sin(q\eta s)\sinh(q\epsilon s)} - \frac{1}{s^2} + \frac{q^2(\epsilon^2-\eta^2)}{6} \;. \tag{98}$$

Therefore, the Lagrangian $\mathscr{L}^{(2)}$ can now be written as (using the symmetry of $K(s,s')$ under $s \to s'$)

$$\mathscr{L}^{(2)} = \frac{iq^2}{128\pi^4}\int_0^\infty ds \int_0^s ds'\ e^{-i(s+s')(m^2-i\epsilon)}\left(K(s,s') - \frac{K_0(s)\ e^{is'(m^2-i\epsilon)}}{s'}\right) + \frac{iq^2}{128\pi^4}\int_0^\infty ds \int_{s_0}^s ds'\ e^{-is(m^2-i\epsilon)}\frac{K_0(s)}{s'} \tag{99}$$

We have introduced a lower bound s_0 to the second integral on the right hand side to regulate the logarithmic divergence in the integral. Performing the s' integral in the second term of the RHS gives us

$$\int_0^\infty ds \int_{s_0}^s ds'\ e^{-is(m^2-i\epsilon)}\frac{K_0(s)}{s'} = \int_0^\infty ds\ e^{-is(m^2-i\epsilon)}K_0(s)\ \log\left(i\gamma m^2 s\right) - \log\left(i\gamma m^2 s_0\right)\int_0^\infty ds\ e^{-is(m^2-i\epsilon)}K_0(s) \;. \tag{100}$$

Also, we can show by integration by parts, we can show that

$$\begin{aligned}\int_0^\infty ds\ e^{-is(m^2-i\epsilon)}K_0(s) &= \frac{3m^2}{2}\int_0^\infty ds\ e^{-is(m^2-i\epsilon)}\mathscr{L} \\ &= C\frac{\partial \mathscr{L}^{(1)}}{\partial m^2} \;.\end{aligned} \tag{101}$$

where C is a calculable constant. Again, this term can be used to renormalize the bare mass of the electron and we can therefore ignore it. Therefore, we finally get our answer to be

$$\boxed{\begin{aligned}\mathscr{L}^{(2)} = \frac{iq^2}{128\pi^4}\int_0^\infty ds\int_0^s ds'\; e^{-i(s+s')(m^2-i\epsilon)}\left(K(s,s') - \frac{K_0(s)\; e^{is'(m^2-i\epsilon)}}{s'}\right)\\ + \frac{iq^2}{128\pi^4}\int_0^\infty ds\; e^{-is(m^2-i\epsilon)}K_0(s)\left(\log\big(i\gamma m^2 s\big) - \frac{7}{6}\right).\end{aligned}} \tag{102}$$

where we subtract the $7/6$ as a convention for mass renormalization. For clarity, let us rewrite the functions $K(s,s')$ and $K_0(s)$–

$$\begin{aligned}K(s,s') = \frac{(q\eta)^2(q\epsilon)^2}{\sin(q\eta s)\sin(q\eta s')\sinh(q\epsilon s)\sinh(q\epsilon s')}\left(m^2 J_0 + \frac{iJ}{2}\right) - \\ \frac{1}{ss'(s+s')}\left[m^2\left(1-\frac{q^2}{6}(\epsilon^2-\eta^2)(s^2+s'^2+ss')\right) + \frac{i}{s+s'}\left(1-\frac{11q^2}{6}(\epsilon^2-\eta^2)ss'\right)\right]\end{aligned} \tag{103}$$

$$\begin{aligned}K_0(s) = \frac{(q\eta)(q\epsilon)}{\sin(q\eta s)\sinh(q\epsilon s)}\left(m^2 + \frac{i}{2}\left(q\eta\;\cot(q\eta s) + q\epsilon\;\coth(q\epsilon s)\right)\right) - \\ \frac{1}{s^2}\left(m^2 - \frac{qm^2}{6}(\epsilon^2-\eta^2)s^2 + \frac{i}{s}\right)\end{aligned} \tag{104}$$

This is extremely complicated! It turns out that this expression simplifies a little bit when $\epsilon \to 0$.

<u>**Simplification for one-field case**</u>

The expression for the case of a magnetic field background simplifies considerably by taking $\eta = B$ and $\epsilon = 0$. We make the variable change

$$t = s + s' \tag{105a}$$

$$u = \frac{s'}{s+s'}\;. \tag{105b}$$

We also substitute $s \to s/qB$ and $s' \to s'/qB$. We will calculate different quantities under this variable change.

<u>$K(s,s')$</u>

The expression for $K(s,s')$ consists of J, J_0, and subtracted divergent terms, multiplied by the prefactor. We will calculate these terms individually:-

1. $\underline{J_0}$: To calculate J_0, we need to know what a and b are. In the limit $\epsilon \to 0$, a and b are given by

$$a = qB(\cot(s) + \cot(s')) \tag{106a}$$
$$b = \frac{qB}{s} + \frac{qB}{s'} \ . \tag{106b}$$

Therefore, in terms of t and u, J_0 is given by

$$J_0 = \frac{\sin(tu)\sin(t(1-u))}{qtb_s} \frac{1}{a_s - b_s} \log\left(\frac{a_s}{b_s}\right) \ , \tag{107}$$

where a_s and b_s are given by

$$a_s = \frac{\sin(tu)\sin(t(1-u))}{t^2 u(1-u)} \tag{108a}$$
$$b_s = \frac{\sin(t)}{t} \ . \tag{108b}$$

2. $\underline{J}$: In the limit $\epsilon \to 0$, we have that

$$p = 2(qB)^2(\cot(s)\cot(s') + 3) \tag{109a}$$
$$q = \frac{2(qB)^2}{ss'} \ . \tag{109b}$$

Therefore, J is given by

$$J = \frac{2\sin(tu)\sin(t(1-u))}{t^2(a_s - b_s)} \left[\frac{a_s - c_s}{a_s - b_s} \log\left(\frac{a_s}{b_s}\right) - \frac{b_s - c_s}{b_s}\right] \ , \tag{110}$$

where c_s is given by

$$c_s = \cos(tu)\cos(t(1-u)) + 3\sin(tu)\sin(t(1-u)) \ . \tag{111}$$

3. <u>leftover terms</u>: In the limit $\epsilon \to 0$, the leftover term is given by

$$\text{lo} = \frac{(qB)^4}{t^3 u(1-u)} \left[\frac{m^2}{qB}\left(1 + \frac{t^2}{6}(u^2 - u + 1)\right) + \frac{i}{t}\left(1 + \frac{11t^2}{6}u(1-u)\right)\right] \ . \tag{112}$$

<u>PF</u>

The prefactor in terms of t and u is given by

$$\text{PF} = \frac{(qB)^4}{t^2 u(1-u)} \frac{1}{\sin(tu)\sin(t(1-u))} \ . \tag{113}$$

$\underline{K_0(s)}$

To calculate $K_0(s)$, we need to calculate $\mathscr{L}(s)$. In the limit $\epsilon \to 0$, $\mathscr{L}$ is given by

$$\mathscr{L}(s) = \frac{qB}{s\sin(qBs)} - \frac{1}{s^2} - \frac{q^2B^2}{6} \; . \tag{114}$$

Therefore, $K_0(s)$ is given by

$$\begin{aligned} K_0(s) &= \left(m^2 - \frac{i}{2}\frac{\partial}{\partial s}\right)\mathscr{L} \\ &= m^2\left[\frac{qB}{s\sin(qBs)} - \frac{1}{s^2} - \frac{q^2B^2}{6}\right] - \frac{i}{2}\left[\frac{2}{s^3} - \frac{qB}{s^2\sin(qBs)} - \frac{(qB)^2\cot(qBs)}{s\sin(qBs)}\right] \; . \end{aligned} \tag{115}$$

In the term of $K_0(s)/s'$, we won't change the variable to t and u defined earlier. Instead, we make the variable change $s \to s/qB$ and $s' \to s'/qB$ followed by $s \to t$ and $s' \to tu$. Under this variable change, $K_0(s)/s'$ is given by

$$\frac{K_0(s)}{s'} = \frac{(qB)^4}{tu}\left[\frac{m^2}{qB}\left(\frac{1}{t\sin(t)} - \frac{1}{t^2} - \frac{1}{6}\right) - \frac{i}{2}\left(\frac{2}{t^3} - \frac{1}{t^2\sin(t)} - \frac{\cot(t)}{t\sin(t)}\right)\right] \; . \tag{116}$$

Now, we combine the answer together. We will separate the answer into three integrals similar to the spinor case [20] such that

$$\mathscr{L}^{(2)}_{\text{1-PI}} = \int_0^\infty \frac{dt}{t^3}\, e^{-im^2t/qB}(T_1 + T_2 + T_3) \; . \tag{117}$$

<u>T_1</u>

This is the term which is proportional to m^2. It is given by

$$T_1 = \frac{m^2 t}{2qB}\int_0^1 \frac{du}{u(1-u)}\left[\frac{1}{a_s - b_s}\log\left(\frac{a_s}{b_s}\right) + \frac{t^2}{6}u(1-u) - \frac{t}{\sin(t)}\right] \; . \tag{118}$$

<u>T_2</u>

This is the term that is proportional to i. It is given by

$$T_2 = \frac{i}{2}\int_0^1 \frac{du}{u(1-u)}\left[\frac{a_s - c_s}{(a_s - b_s)^2}\log\left(\frac{a_s}{b_s}\right) - \frac{b_s - c_s}{b_s(a_s - b_s)} - \frac{11t^2}{6}u(1-u) - \frac{t(1 + t\cot(t))}{2\sin(t)}\right] \; . \tag{119}$$

<u>T_3</u>

This is the remaining term which is not an integral. We simplify this expression a bit by writing

$$\begin{aligned} &\int_0^\infty dt\; e^{-itm^2/qB}\frac{\partial L}{\partial t}\left(\log\left(i\gamma\frac{m^2 t}{qB}\right) - \frac{7}{6}\right) = \\ &\qquad \frac{im^2}{qB}\int_0^\infty dt\; e^{-itm^2/qB}\, L\left(\log\left(i\gamma\frac{m^2 t}{qB}\right) - \frac{7}{6}\right) - \int_0^\infty dt\; e^{-im^2t/qB}\frac{L}{t} \; . \end{aligned} \tag{120}$$

Then, T_3 is given by

$$T_3 = \frac{1}{2}\left(i + \frac{3tm^2}{qB}\left(\log\left(\frac{i\gamma tm^2}{qB}\right) - \frac{7}{6}\right)\right)\left(\frac{t}{\sin t} - 1 - \frac{t^2}{6}\right) . \tag{121}$$

When we rotate the contour to the negative imaginary axis (which is the same as substituting $t \to -it$) and redefine T_1, T_2, and T_3, we get that

$$\mathscr{L}^{(2)}_{\text{1-PI}} = \frac{q^2(qB)^2}{256\pi^4}\int_0^\infty \frac{dt}{t^3}\, e^{-tm^2/qB}(T_1 + T_2 + T_3) , \tag{122}$$

where T_1, T_2 and T_3 are given by

$$T_1 = -\frac{m^2 t}{qB}\int_0^1 \frac{du}{u(1-u)}\left[\frac{1}{a_s - b_s}\log\left(\frac{a_s}{b_s}\right) - \frac{t^2}{6}u(1-u) - \frac{t}{\sinh(t)}\right] , \tag{123}$$

$$T_2 = \int_0^1 \frac{du}{u(1-u)}\left[\frac{a_s - c_s}{(a_s - b_s)^2}\log\left(\frac{a_s}{b_s}\right) - \frac{b_s - c_s}{b_s(a_s - b_s)} + \frac{11t^2}{6}u(1-u) - \frac{t(1 + t\coth(t))}{2\sinh(t)}\right] , \tag{124}$$

$$T_3 = \left(1 - \frac{3tm^2}{qB}\left(\log\left(\frac{\gamma tm^2}{qB}\right) - \frac{7}{6}\right)\right)\left(\frac{t}{\sinh t} - 1 + \frac{t^2}{6}\right) , \tag{125}$$

where

$$a_s = \frac{\sinh(tu)\sinh(t(1-u))}{t^2 u(1-u)} \tag{126a}$$

$$b_s = \frac{\sinh(t)}{t} \tag{126b}$$

$$c_s = \cosh(tu)\cosh(t(1-u)) - 3\sinh(tu)\sinh(t(1-u)) . \tag{126c}$$

2.2.3 2-loop 1-PR diagram

Unlike the 2-loop 1-PI case, the 1-PR diagram can be calculated with much more ease. The 2-loop 1-PR expression is given by (for $\epsilon \to 0$)

$$\mathscr{L}^{(2)}_{\text{1-PR}} = \frac{q^4 B^2}{1024\pi^4} I_2^2 . \tag{127}$$

Here, I_2 denotes the derivative of the 1-loop integral and is given by

$$I_2 = \int_0^\infty \frac{ds}{s^3}\, e^{-m^2 s/qB}\left[\frac{s}{\sinh s} - \frac{s^2}{\sinh s \tanh s} + \frac{s^2}{3}\right] . \tag{128}$$

Using the same technique we used in Sec 2.2.1, we can find a closed form for I_2–

$$I_2 = -4\zeta_H\left(-1, \frac{1 + m^2/qB}{2}\right) - 8\zeta_H'\left(-1, \frac{1 + m^2/qB}{2}\right) + 2\left(\frac{m^2}{qB}\right)\zeta_H'\left(0, \frac{1 + m^2/qB}{2}\right) - \frac{1}{3}\log\left(\frac{m^2}{2qB}\right) . \tag{129}$$

2.3 Padé-Borel reconstruction

In this section, we will detail how one can reconstruct an asymptotic series using the Padé-Borel method. There are three steps involved in constructing the Padé-Borel summation—Borel transform, Padé-approximation, and Laplace transform.

Let us consider the asymptotic series $\mathscr{S}$ with the coefficients a_n–

$$\mathscr{S}(z) = \sum_{n=0}^{\infty} a_n z^{2n} \,, \tag{130}$$

where the factorial divergence is of the form

$$a_n \sim \sum_{\mathscr{P}=1}^{\infty} C_{\mathscr{P}}\, A_{\mathscr{P}}^{-2n-k_{\mathscr{P}}-1}\, \Gamma(2n+k_{\mathscr{P}}+1) + \text{corr.} \,,\; n \to \infty \,. \tag{131}$$

Here, $k_{\mathscr{P}}$ is a fixed constant. Every successive term in the sum of eq. (131) is exponentially smaller than the next, since $A_1 < A_2 < A_3 \ldots$ and we refer to them as "power-law contributions" [13]. Using this power series, we will define the quantites required for the reconstruction:

1. Borel transform: A general Borel transform $\widehat{\mathscr{S}}_{p,N^*}$ is defined as

   $$\widehat{\mathscr{S}}_{p,N^*}(z) = \sum_{n=0}^{N^*} \frac{a_n}{(2n+p)!}\, z^{2n+p} \,,\; p \geq 0 \,, \tag{132}$$

   that is, we simply remove the factorial divergence of the coefficient a_n in eq. (131) by simply dividing by a factorial. The resulting series is convergent with radius of convergence $R = A_1$.

2. Padé approximant: In order to analytically continue the Borel transform series outside its radius of convergence, we will use a Padé approximant. A Padé approximant P_M^N is a rational function that is constructed such that it has the same perturbative expansion as the Borel transform inside its radius of convergence–

   $$P_M^N[\widehat{\mathscr{S}}](z) \equiv \frac{U_0 + U_1 z + \cdots + U_N z^N}{1 + D_1 z + \ldots D_M z^M} \sim \sum_{n=0}^{N^*} \frac{a_n}{(2n+p)!} z^{2n+p} \equiv \widehat{\mathscr{S}}_{p,N^*}(z) \,,\; z \to 0 \,, \tag{133}$$

   where N^* denotes the number of coefficients required to construct P_M^N (N^* will depend on N, M and p). The Padé approximant used for most applications is the "diagonal Padé approximant", for which $N = M$. However, we will investigate the effect on the reconstruction when the Padé approximant deviates from the diagonal approximant. We will parametrize this deviation by f, where $M = N + f$.

3. Padé-Borel transform: The Padé-Borel transform is now defined as

$$\mathrm{PB}_{N,f,p}\left[\mathscr{S}\right](z) = z^{-p}\int_0^\infty dt\; e^{-t}\; P^N_{N+f}\left[\widehat{\mathscr{S}_{p,N*}}\right](zt)\,. \tag{134}$$

This Padé-Borel transform is asymptotic to the original series $\mathscr{S}$ as $z \to 0$ [1]. This integral can be rewritten in terms of the complex variable ζ by doing a variable change $\zeta = zt$ such that

$$\mathrm{PB}_{N,f,p}\left[\mathscr{S}\right](z) = z^{-p-1}\int_0^{\infty e^{i\theta}} dt\; e^{-\zeta/z}\; P^N_{N+f}\left[\widehat{\mathscr{S}_{p,N^*}}\right](\zeta)\,, \tag{135}$$

where θ is the argument of the complex variable z.

The Borel transform of an asymptotic series is usually characterized by singularities in its analytical continuation (outside the radius of convergence). These singularities are signs of the sector of instability we mentioned earlier and leads to non-perturbative contributions to the asymptotic series that we called trans-series. In our case, all these singularities will lie along a single line in the complex plane of ζ. This line is known as the "Stoke's line". We cannot perform the integration in eq. (134) when the integration contour approaches this line. In this case, we rotate the contour infinitesimally away from the Stokes line. This is called a 'lateral Borel transform". This is depicted in fig. 3. The two lateral Borel transforms PB^{θ^+} and PB^{θ^-} differ in value by a non-perturbative contribution obtained by performing a contour integration around each of the singularities on the Stoke's line.

In fact, it turns out that there is a direct relation between the large order behaviour in eq. (131) of an asymptotic series and the non-perturbative terms it generates. This relation is known as the "Borel dispersion relation". As the procedure to obtain this dispersion relation is relatively well-known and we only need the result in order to conduct our analysis, we will state the result and refer to [2, 9] for the derivation. For an asymptotic series in eq. (130) with coefficients with large order behaviour in eq. (131), the non-perturbative contribution to the lateral Borel transform is given by

$$\mathrm{Im}\,\mathscr{S}(z) = \sum_{\mathscr{P}=1}^{\infty} \frac{i\pi C_{\mathscr{P}}}{2(z)^{k_{\mathscr{P}}+1}}\; e^{-A_{\mathscr{P}}/|z|} + \text{corr.}\,, \tag{136}$$

where $\arg z = \theta$. In our example the Stokes line will mostly lie on the imaginary axis, i.e., $\theta = \pm\pi/2$.

In Sec. 3 , we will use the Padé-Borel reconstruction to reconstruct functional approximations to the exact EHL using different parameter values of f and p. We will find out the

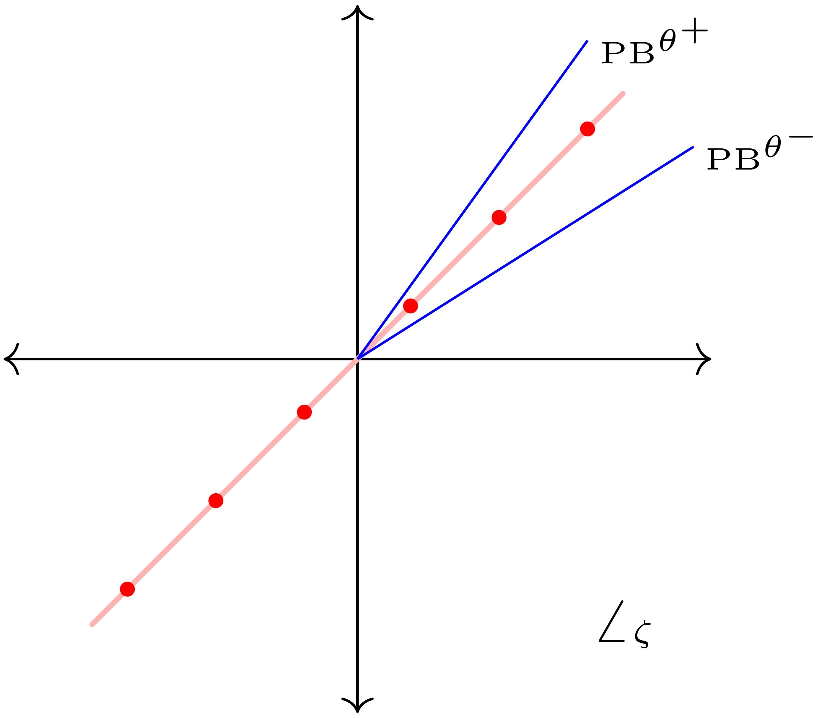

Figure 3: The Pink line is the Stoke's line. This line of singularities can be avoided in two ways, giving rise to two values of lateral Borel transforms— PB^{θ^+} and PB^{θ^-}.

most optimal values of f and p by comparing the functional approximations to either the exact function or numerical approximations. In addition, we will use the Borel-dispersion relation to find out the non-perturbative behaviour of the EHLs and hence demonstrate how the trans-series structure of a resurgent function is intricately linked to the large order behaviour of its perturbative coefficients.

3 Results and Discussion

We will apply the Padé-Borel reconstruction method to the one-field EHL of sQED for 1-loop and 2-loop, and to the two-field EHL of QED for 1-loop. We will additionally study the resurgent structure and trans-series structures for each of these cases.

3.1 1-loop sQED EHL

This section is divided into three parts— first, we will construct the Padé-Borel resummed function for the 1-loop sQED EHL in the constant magnetic field limit. Then, we will do the same for a constant electric field using an analytic continuation of the magnetic field case. In the last part, we will study the trans-series structure of the EHL function.

Magnetic field reconstruction

The 1-loop sQED EHL is given by

$$\mathscr{L}^{(1)}_{\mathrm{sQED}}(qB,m^2) = \frac{q^2B^2}{16\pi^2}\int_0^\infty \frac{dt}{t^2}\, e^{-m^2t/qB}\left[\frac{1}{\sinh t}-\frac{1}{t}+\frac{t}{6}\right] . \tag{137}$$

It was shown by Weisskopf in 1936 [14] that the 1-loop sQED EHL can be expressed in terms of the QED EHL–

$$\mathscr{L}^{(1)}_{\mathrm{sQED}}(qB,m^2) = \frac{1}{2}\mathscr{L}^{(1)}_{\mathrm{QED}}(qB,m^2) - \frac{1}{4}\mathscr{L}^{(1)}_{\mathrm{QED}}(qB,2m^2) , \tag{138}$$

using the identity $1/\sinh t = \coth(t/2) - \coth(t)$. It might seem that because the EHLs of QED and sQED follow this simple relation, the resurgent structure for both cases would be similar. However, it turns out that this is not true and the EHL of sQED has a spurious pole structure that is not noticed in the case of the QED EHL. It seems that resurgent structures are not conserved in simple binary operations. We will provide more proof of this as we go on in this section.

The weak-field expansion for eq. (137) is given by

$$\mathscr{L}^{(1)}_{\mathrm{sQED}}(qB,m^2) \sim \frac{m^4}{4\pi^2}\left(\frac{qB}{m^2}\right)^4 \sum_{n=0}^{\infty} a_n^{(1)}\left(\frac{qB}{m^2}\right)^{2n} \equiv \frac{m^4}{4\pi^2}\left(\frac{qB}{m^2}\right)^4 \mathscr{S}^{(1)}_{\mathrm{sQED}}(qB/m^2) \; , \; \frac{qB}{m^2}\to 0 \, , \tag{139}$$

where the coefficients $a_n^{(1)}$ may be found exactly, and have the form

$$a_n^{(1)} = (-1)^n \frac{2^{2n+3}-1}{(2\pi)^{2n+4}}\, \zeta(2n+4)\,(2n+1)! \, , \tag{140}$$

and the zeta function is defined as $\zeta(\nu) = \sum_{n=1}^{\infty} 1/n^{\nu}$.

The Borel transform for the series $\mathscr{S}^{(1)}$ is given by (we will omit the transcript sQED as it is clear from the context that we are talking about sQED)

$$\widehat{\mathscr{S}}^{(1)}_{p,N^*}(g_B) = \sum_{n=0}^{N^*} \frac{a_n^{(1)}}{(2n+p)!}\, g_B^{2n+p} \; , \; p\geq 0 \, , \tag{141}$$

where we have defined $g_B = qB/m^2$, a dimensionless measure of the strength of the external magnetic field. The Padé-Borel reconstruction is then given by

$$\mathrm{PB}_{N,f,p}\left[\mathscr{S}^{(1)}\right](g_B) = g_B^{-p}\int_0^\infty dt\; e^{-t}\, P^N_{N+f}\left[\widehat{\mathscr{S}}^{(1)}_{p,N^*}\right](g_B t) \, . \tag{142}$$

To test this functional approximation, we compare this Padé-Borel reconstruction with the exact form in eq. (48) in fig. 4. It is very apparent that the Padé-Borel reconstruction gives an remarkable functional approximation even for as little perturbative information as $N = 2$.

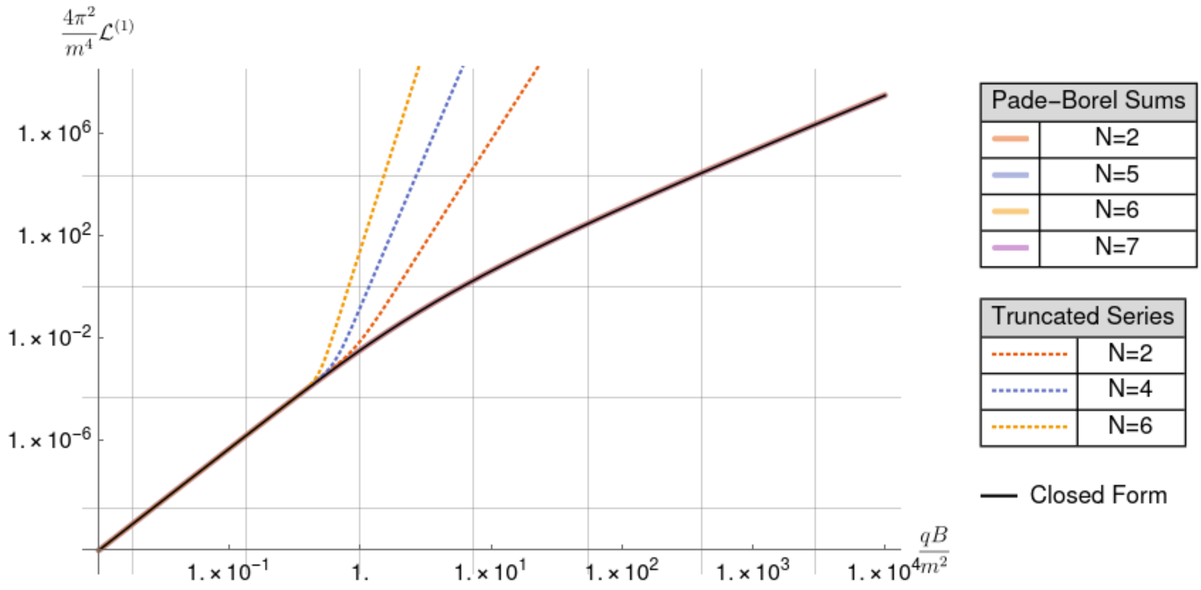

Figure 4: A depiction of the efficacy of the Padé-Borel reconstruction to give a functional approximation for the 1-loop sQED EHL in a constant magnetic field background. The Padé-Borel reconstructions are able to give remarkably accurate functional approximations to the original function even for $N = 2$, in contrast with using a truncated version of the asymptotic series in eq. (139) which diverges very quickly from the original function. The parameter values used here are $p = 1$, $f = 1$.

In order to choose the best parameter values for the reconstruction, we also compare reconstructions with different parameter values f and p with the closed form in fig. 5. Notice that all the reconstructions are equivalent in their approximations upto field values of around $g_B \sim 10$, after which they diverge. This is an indication of there being a non-perturbative difference in Padé-Borel resummations with different parameter values. This is to be expected, because it can be easily be proved by integration of parts that all the Laplace transforms of the Borel transforms $\widetilde{\mathscr{F}}^{(1)}_{p,N^*}$ are equivalent for $p \geq 0$ inside the radius of convergence of the Borel transform which, in this case, is $R = \pi$. Therefore, the different reconstructions can only differ in the non-perturbative function $e^{-\pi/g_B}$.

From fig. 5, it is obvious that the best approximation is given by the parameter values $p = 1$ and $f = 1$. The efficacy of these parameter values is not arbitrary; in fact it can be predicted by looking at the large field behaviour of the EHL. It can be proved [14, 21] that the large order behaviour of the 1-loop sQED EHL is given by

$$\mathscr{L}^{(1)}_{\text{sQED}} \sim \frac{q^2B^2}{96\pi^2} \log\left(\frac{qB}{m^2}\right) , \quad \frac{qB}{m^2} \to \infty . \tag{143}$$

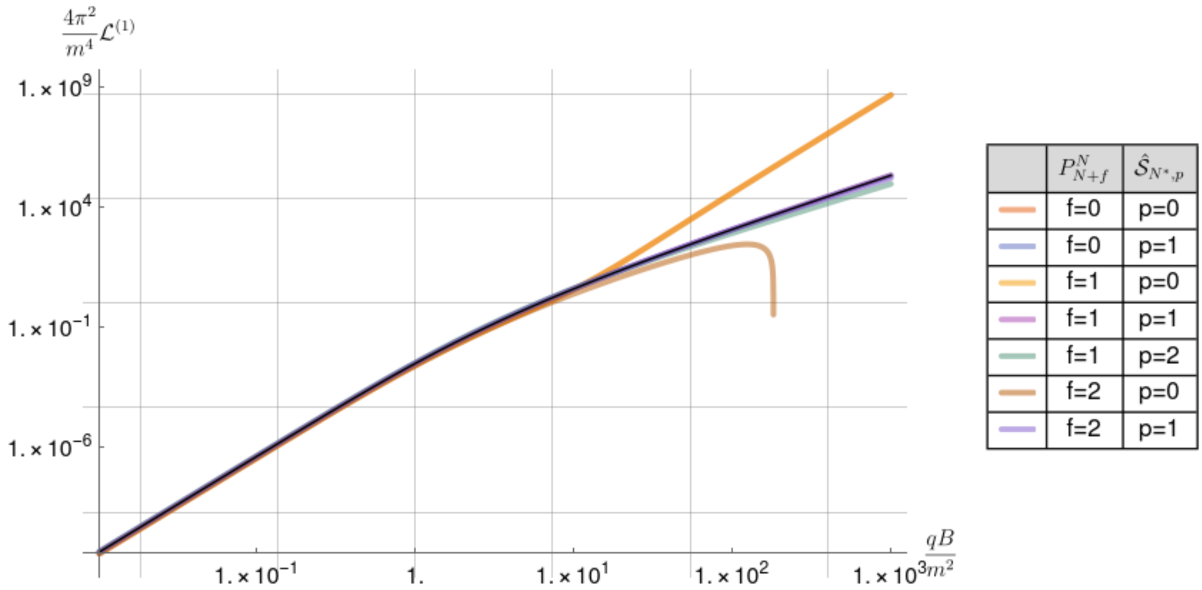

Figure 5: Comparison of different parameter values f and p in their ability to reconstruct the original 1-loop EHL for sQED. It is apparent that the $p = 1$, $f = 1$ (the magenta line) provides the best approximation.

On the other hand, the large field behaviour of $\mathrm{PB}_{N,f,p}$ is given by

$$\frac{m^4}{4\pi^2}\left(\frac{qB}{m^2}\right)^4 \mathrm{PB}_{N,f,p}\left[\mathscr{S}^{(1)}\right](g_B) \sim \frac{m^4}{4\pi^2}\left(\frac{qB}{m^2}\right)^{4-p} \int_{1/g_B}^{\infty} dt\; e^{-t}\, \frac{U_N/D_{N+f}}{(g_B t)^f}\;, \quad g_B \to \infty\,, \tag{144}$$

where U_N and D_{N+f} are the coefficients of the N^{th} and $(N+f)^{\text{th}}$ degree terms in the numerator and denominator of the Padé-approximant as defined in eq. (133). The infrared region of the integral $[0, 1/g_B)$ may be ignored in the strong-field limit as it will be $\mathscr{O}(1/g_B)$. The integral in eq. (144) is the incomplete Gamma function $\Gamma(-f+1, x)$ with $x = 1/g_B$, which is defined as

$$\Gamma(a,x) = \int_x^{\infty} dt\; e^{-t}\, t^{a-1}\,. \tag{145}$$

The derivative of the incomplete Gamma function, $\partial_x\Gamma(-f+1,x) = -\frac{e^{-x}}{x^f}$, can be expanded in the limit $x \to 0$ to deduce that, up to a multiplicative constant, we would have

$$\frac{m^4}{4\pi^2}\left(\frac{qB}{m^2}\right)^4 \mathrm{PB}_{N,f,p}\left[\mathscr{S}^{(1)}\right] \sim \frac{m^4}{4\pi^2}\left(\frac{qB}{m^2}\right)^{4-p} \begin{cases} \frac{g_B^{f-1}}{g_B^f}, & \text{if } f > 1 \\ \frac{\log g_B}{g_B} & \text{if } f = 1 \end{cases}\;, \quad \frac{qB}{m^2} \to \infty\,. \tag{146}$$

From the above discussions, we deduce that the optimal parameter choices would be $p = 1$ and $f = 1$. We notice through this example that the Padé-Borel reconstruction results in a family of solutions, parameterized by f and p, that differ in their non-perturbative behaviour. A very effective Padé-Borel resummation can be constructed if we have access to some data regarding how the function behaves in the large field limit.

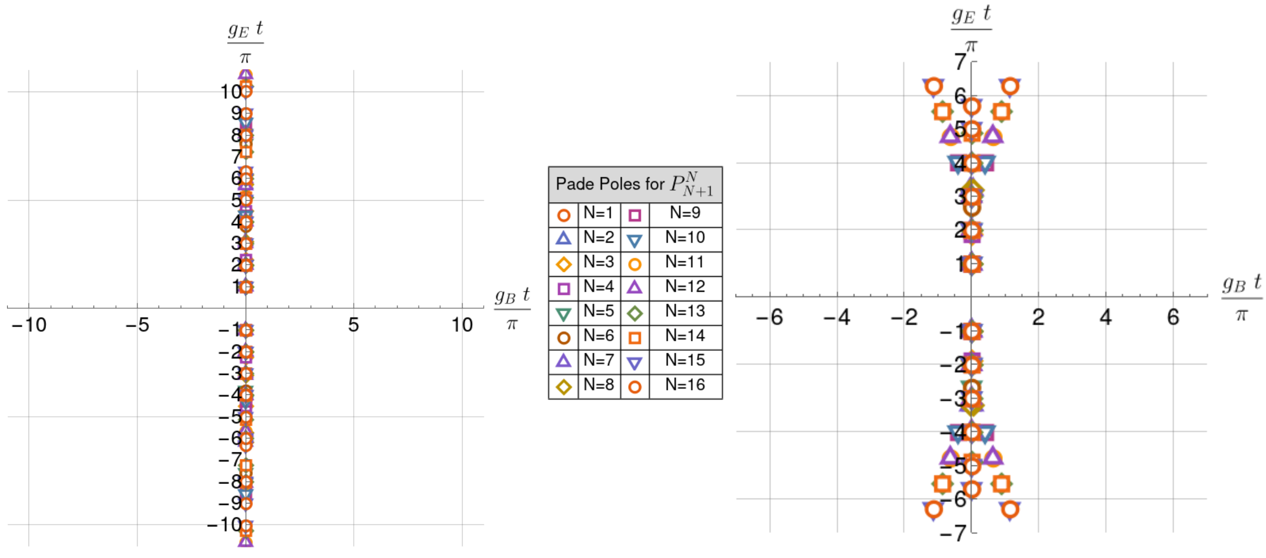

(a) (b)

Figure 6: Poles of the Padé approximants of the 1-loop EHL constructed in two different ways. A naive construction of Padé approximants leads to arcs of spurious poles as seen in fig. 6b, whereas Padé-like approximants constructed from the spinor 1-loop EHL do not give rise to such spurious poles, as is seen in fig. 6a.

Electric field reconstruction

To reconstruct the EHL for a constant electric field background, we do the variable change $B \to -iE$ (refer to [9] for an explanation for why this is the correct choice). However, when we plot the poles of the Padé approximants of the Borel transform $\widehat{\mathscr{F}}^{(1)}(\zeta)$, as we have in fig. 6, we find that the singularities of the Borel transform lie on the imaginary axis, making the Laplace transform in eq. (135) undefined for electric field backgrounds. As we described before, we will have to use a lateral Borel transform in order to solve this problem.

The poles of $\widehat{\mathscr{F}}^{(1)}$ are at integer multiples of π. This is very much expected because of the form of the integrand in eq. (137), as $\sinh t$ has poles on the imaginary axis at integral multiples of π. Notice that when the poles of the Padé transform of $\widehat{\mathscr{F}}^{(1)}$ are plotted, we notice a collection of spurious poles in arcs around the imaginary axis. However, when the relation in eq. (138) is used to construct Padé-like approximants, these spurious poles are absent. This is preliminary evidence for resurgent functions changing properties under the linear operation of addition. These arcs of spurious poles have been studied before in literature and are known as “Szegő curves” [22–24].

To perform the lateral Borel transform, we will choose PB^{θ^-}. After this, we will rotate the

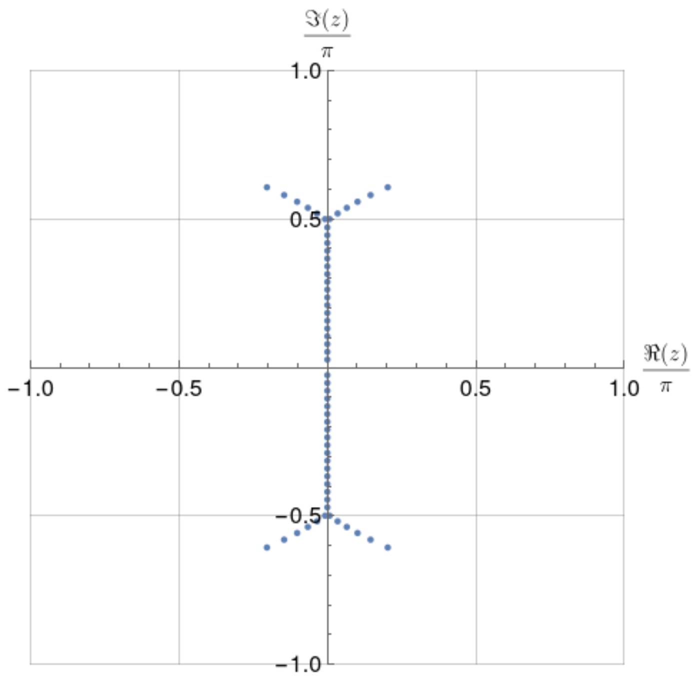

Figure 7: The poles of the normalized Padé approximant $P_{61}^{60}(120z)$ illustrating the Szegő curves. The plot shows the characteristic curve of the spurious poles of a normalized partial sum $s_n(nz)$.

contour of integration such that we get that

$$\mathrm{PB}_{N,f,p}\left[\mathscr{S}^{(1)}\right](g_E) = \frac{1}{(-ig_E)^{p+1}} \int_0^\infty dt\, e^{-it/g_E}\, P_{N+f}^{N}\left[\widehat{\mathscr{S}}_{N^*,p}^{(1)}\right](t)\,, \tag{147}$$

where $g_E = qE/m^2$. This integral will have both a real and an imaginary part. Therefore, an analytical continuation to electric fields gives rise to an imaginary contribution to the EHL. This imaginary contribution is responsible for the false vacuum decay that leads to Schwinger pair production [11]. The instability of the vacuum in the presence of strong electric fields leads to the production of charged particle and anti-particle pairs and hence causes vacuum polarization. This effect is entirely non-perturbative and is suppressed by a factor of $e^{-\pi m^2/qE}$. Therefore, effects such as these cannot be probed by conventional perturbative analysis methods and require methodologies developed in the Resurgence program.

We will now use the Padé approximants we constructed for the case of constant magnetic field background to reconstruct the EHL for electric field backgrounds using eq. (147). The results of this approximation are given in fig. 8 and fig. 9 . Clearly, the Padé-Borel transform is very effective in reconstructing both the real and imaginary parts of the EHL, even though the imaginary part is completely non-perturbative in nature, and the Padé-Borel transform is constructed by only using very limited amount of perturbative data.

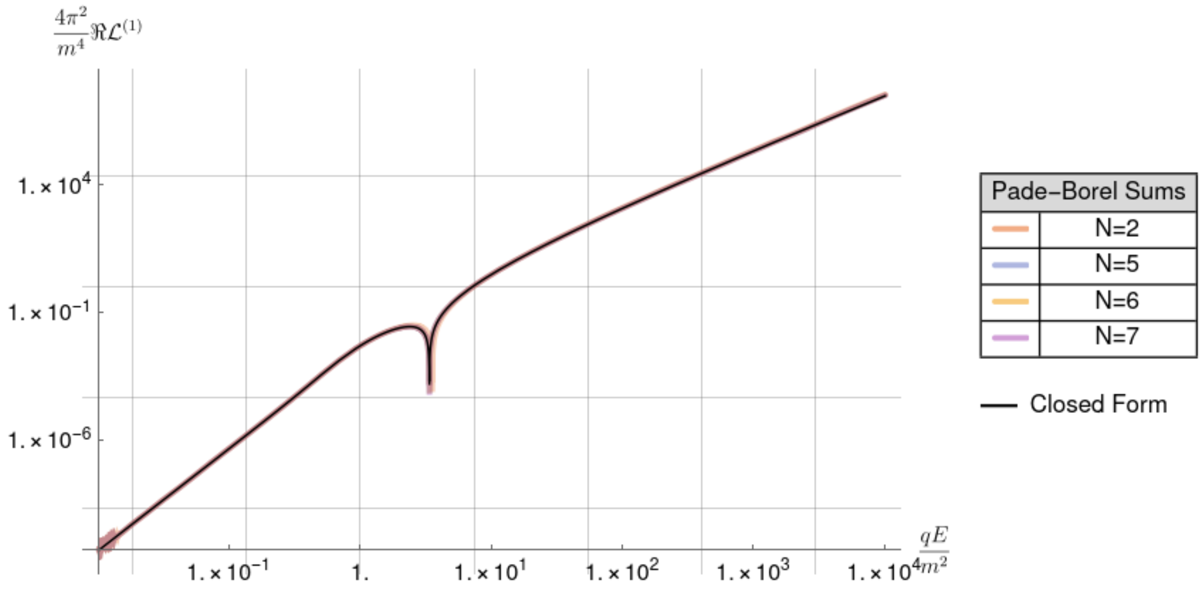

Figure 8: Real part of the Padé-Borel reconstruction of the 1-loop sQED EHL for constant electric field background. The parameter values used are $p = 1$, $f = 1$.

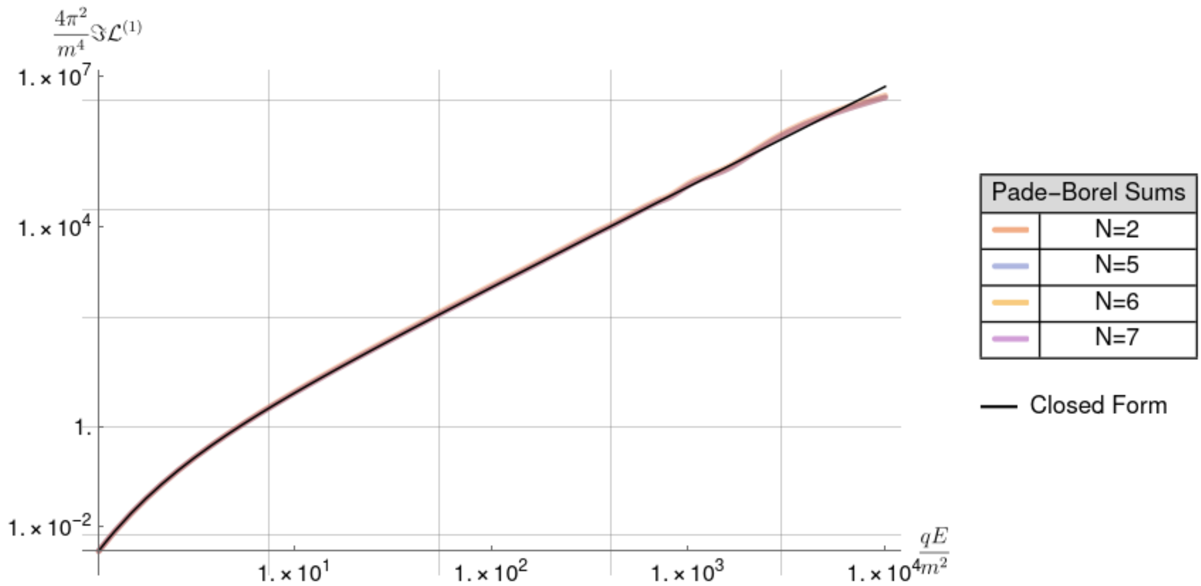

Figure 9: Imaginary part of the Padé-Borel reconstruction of the 1-loop sQED EHL for constant electric field background. The parameter values used are $p = 1$, $f = 1$. Notice that the Padé-Borel resummation is able to reconstruct the imaginary part of the EHL almost exactly, even though the imaginary part is non-perturbative in nature.

Trans-Series Structure

As we mentioned earlier, the non-perturbative behaviour of a resurgent function is related to the large-order behaviour of the coefficients of its perturbative expansion via the Borel dispersion relation in eq. (136). Let us verify this for the case of the 1-loop sQED EHL. The large order behaviour of the weak-field coefficients by expanding $\zeta(2n+4)$ to get that

$$a_n^{(1)} \sim (-1)^n \frac{2^{2n+3}-1}{(2\pi)^{2n+4}} \Gamma(2n+2) \left[1 + \frac{1}{2^{2n+4}} + \frac{1}{3^{2n+4}} + \dots\right] , \; n \to \infty . \tag{148}$$

Now, using eq. (136), we deduce that

$$\mathrm{Im}\, \mathscr{L}^{(1)}_{\mathrm{sQED}} = \frac{m^4}{16\pi^3} \left(\frac{qE}{m^2}\right)^2 \left[e^{-m^2\pi/qE} - \frac{1}{4} e^{-2m^2\pi/qE} + \frac{1}{9} e^{-3m^2\pi/qE} + \dots\right] . \tag{149}$$

This is exactly the expression initially obtained by Schwinger for the rate of pair production. In fact, it was noted that the negative terms of even terms in eq. (149) signify the corrections to pair production due to Bose attraction [20]. On the other hand, the rate of Schwinger pair production is higher for fermions in case of QED because of Fermi repulsion. In terms of Resurgence, each successive exponentially small term arises from successive instanton corrections, which in turn arises from successive points of singularity on the Stoke's line in fig. 3.

3.2 2-loop sQED EHL

We will now look at the 2-loop sQED EHL, which is significantly more complicated to analyse than the 1-loop case. It is in this more complex problem that we'll see the true power of Resurgence and reconstruction methods. We will analyse both the 1-PI and 1-PR diagrams together.

Magnetic field reconstruction

The integral forms for the 1-PI and 1-PR diagrams of the 2-loop sQED EHL in the case of a constant magnetic field background are given in eq. (122) and eq. (127). We will start by doing a weak-field expansion for both of the integral forms–

$$\mathscr{L}^{(2)}_{\text{1-PI}} \sim \frac{q^2 m^4}{256\pi^4} \left(\frac{qB}{m^2}\right)^4 \sum_{n=0}^{\infty} a_n^{(2I)} \left(\frac{qB}{m^2}\right)^{2n} \equiv \frac{q^2 m^4}{256\pi^4} \left(\frac{qB}{m^2}\right)^4 \mathscr{S}^{(2I)}(qB/m^2) , \; \frac{qB}{m^2} \to 0 , \tag{150a}$$

$$\mathscr{L}^{(2)}_{\text{1-PR}} \sim \frac{q^2 m^4}{1024\pi^4} \left(\frac{qB}{m^2}\right)^6 \sum_{n=0}^{\infty} a_n^{(2R)} \left(\frac{qB}{m^2}\right)^{2n} \equiv \frac{q^2 m^4}{1024\pi^4} \left(\frac{qB}{m^2}\right)^6 \mathscr{S}^{(2R)}(qB/m^2) , \; \frac{qB}{m^2} \to 0 . \tag{150b}$$

The closed form of the 2-loop coefficients $a_n^{(2I)}$ and $a_n^{(2R)}$ are not known. In fact, the weak-field coefficients $a_n^{(2I)}$ are significantly heavy to calculate computationally owing to the complexity of the integral in eq. (122). We were able to compute the first 27 coefficients of the 1-PI diagrams following the procedure detailed in [13]. On the other hand, the 1-PR coefficients $a_n^{(2R)}$ are relatively easy to compute and can be calculated upto arbitrary orders. We have tabulated the first few coefficients of the 1-PI and 1-PR diagrams in our work [9]. It is in cases where it is very difficult to compute weak-field coefficients that the program of Resurgence is truly powerful— we need only compute a finite number of coefficients in order to construct effective functional approximations and trans-series structure for the integral function.

As we did for the 1-loop case, we will define the Borel transforms for the 2-loop case as

$$\widehat{S}^{(2I)}_{p,N^*}(g_B) = \sum_{n=0}^{N^*} \frac{a_n^{(2I)}}{(2n+p)!} g_B^{2n+p}\,, \tag{151a}$$

$$\widehat{S}^{(2R)}_{p,N^*}(g_B) = \sum_{n=0}^{N^*} \frac{a_n^{(2R)}}{(2n+p)!} g_B^{2n+p}\,. \tag{151b}$$

and the Padé-Borel reconstructions as

$$\mathrm{PB}_{N,f,p}\left[\mathscr{S}^{(2I)}\right](g_B) = g_B^{-p} \int_0^\infty dt\ e^{-t}\ P^N_{N+f}\left[\widehat{\mathscr{S}}^{(2I)}_{p,N^*}\right](g_B t)\,, \tag{152a}$$

$$\mathrm{PB}_{N,f,p}\left[\mathscr{S}^{(2R)}\right](g_B) = g_B^{-p} \int_0^\infty dt\ e^{-t}\ P^N_{N+f}\left[\widehat{\mathscr{S}}^{(2R)}_{p,N^*}\right](g_B t)\,. \tag{152b}$$

The results for the reconstructions for the 1-PI diagram is given in fig. 10. The best functional approximation is given by the parameter values $f = 1$ and $p = 1$. Like in the 1-loop case, these parameter values can be explained by looking at the large field behaviour of the 2-loop 1-PI contribution, which is given by [15, 21]

$$\mathscr{L}^{(2)}_{\text{1-PI}} \sim \frac{q^4 B^2}{128\pi^4} \log\left(\frac{qB}{m^2}\right)\,, \quad \frac{qB}{m^2} \to \infty\,. \tag{153}$$

While the parameter values for the 1-loop and 2-loop 1-PI match because of similar large field behaviours, the optimal parameters for the 2-loop 1-PR EHL are quite different. The results for the Padé-Borel approximation as compared to the closed form of the 1-PR 2-loop EHL is given in fig. 11. In clear contrast to the other two cases, the parameter values $f = 1$, $p = 3$ are the optimal for the best approximation for $\mathscr{L}^{(2)}_{\text{1-PR}}$. This is because to obtain the large field behaviour [25]

$$\mathscr{L}^{(2)}_{\text{1-PR}} \sim \frac{1}{9}\frac{q^4 B^2}{1024\pi^4} \left[\log\left(\frac{qB}{m^2}\right)\right]^2\,, \quad \frac{qB}{m^2} \to \infty\,, \tag{154}$$

from the large field behaviour of the Padé-Borel transform

$$\frac{q^2 m^4}{1024\pi^4}\left(\frac{qB}{m^2}\right)^6 \mathrm{PB}_{N,f,p}\left[\mathscr{S}^{(2R)}\right] \sim \frac{q^2 m^4}{1024\pi^4}\left(\frac{qB}{m^2}\right)^{6-p} \begin{cases} \frac{g_B^{f-1}}{g_B^f}, & \text{if } f > 1 \\ \frac{\log g_B}{g_B} & \text{if } f = 1 \end{cases}\,, \tag{155}$$

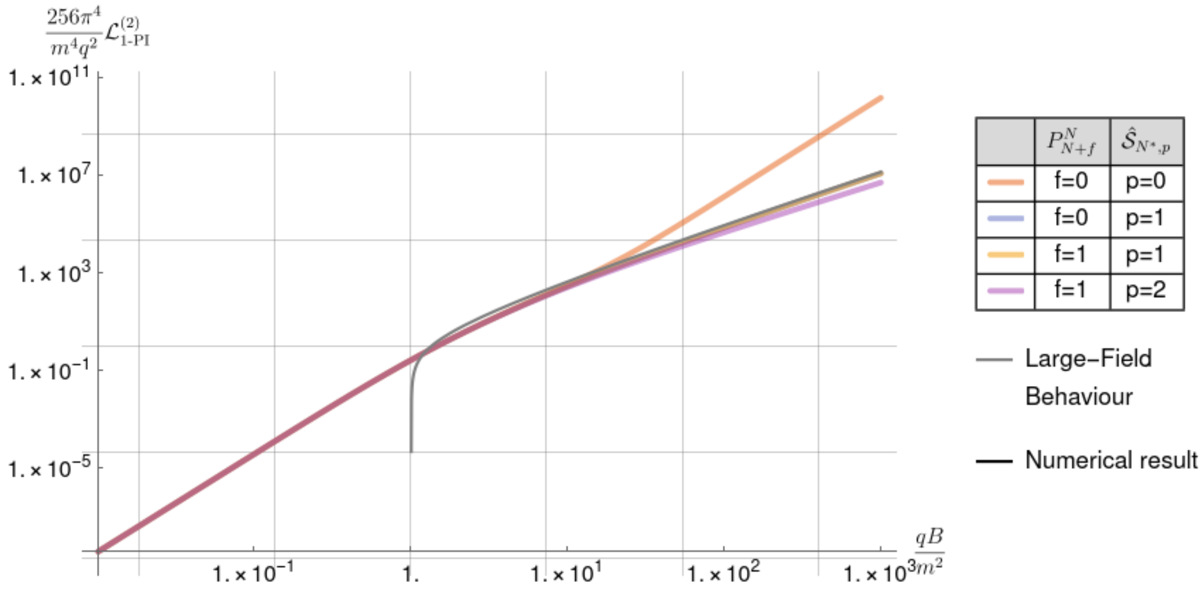

Figure 10: Result of the Padé-Borel reconstruction for the 1-PI diagram of the 2-loop sQED EHL for different parameter values of f and p as compared to numerical integration and large-field behaviour of $\mathscr{L}^{(2)}_{\text{1-PI}}$. Clearly, the parameter values $f=1$, $p=1$ give the optimal functional approximation.

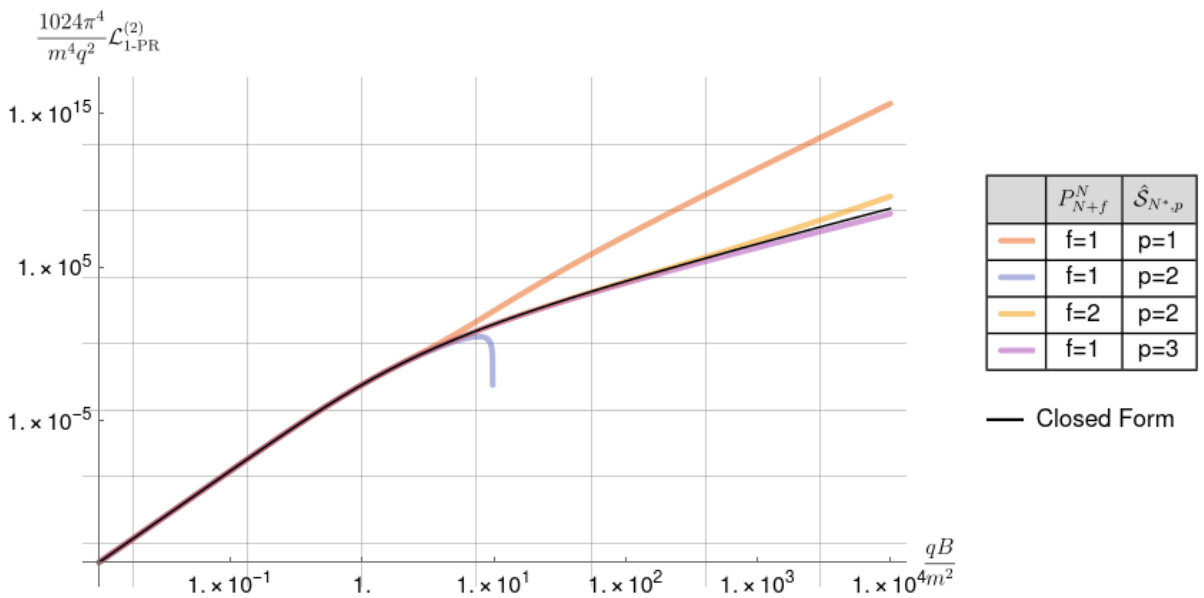

Figure 11: Result of the Padé-Borel reconstruction for the 1-PR diagram of the 2-loop sQED EHL for different parameter values of f and p as compared to numerical integration and large-field behaviour of $\mathscr{L}^{(2)}_{\text{1-PI}}$. Clearly, the parameter values $f=1$, $p=3$ give the optimal functional approximation.

we must have $p=3$, $f=1$.

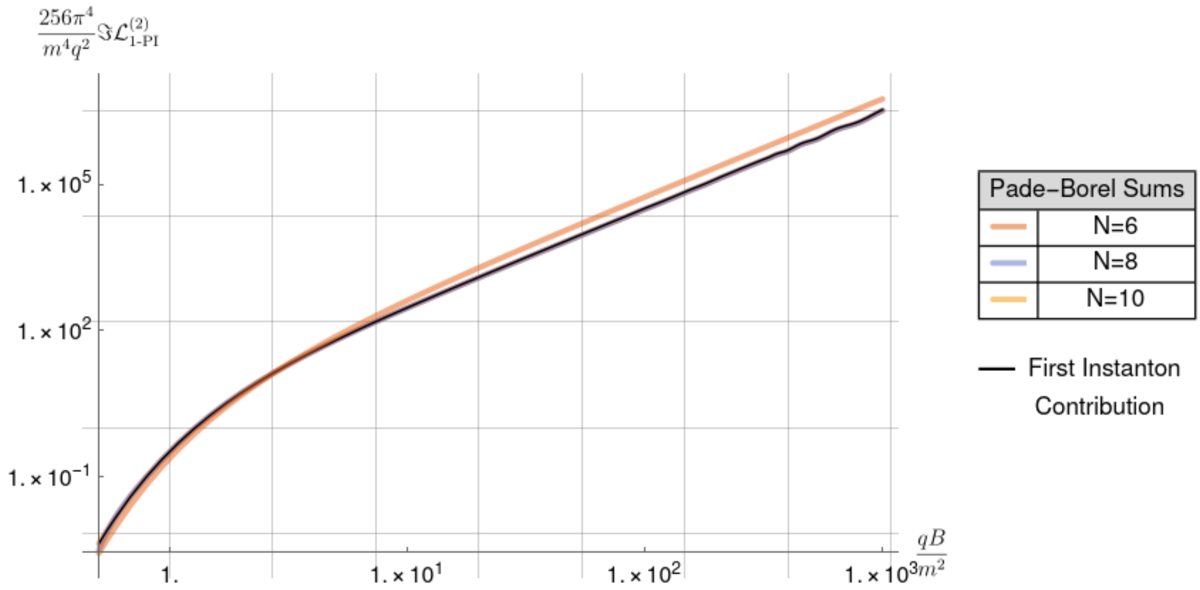

Figure 12: Padé-Borel reconstruction and first instanton contribution to the imaginary part of the 2-loop 1-PI sQED EHL. The first instanton correction is very effective at approximating the imaginary part upto high accuracies.

Electric field reconstruction and trans-series structure

We will do an analytic continuation $B \to -iE$ as we did in the 1-loop case. We have plotted the reconstructed imaginary parts of the 1-PI and 1-PR diagrams in figs. 12 and 13. Although we do not know the instanton contributions that make up the imaginary parts of the 2-loop EHLs in closed form like we did for the 1-loop case (as in eq. (149)), we can still investigate the approximate behaviour of instanton contributions by estimating the large order behaviour of the perturbative coefficients $a_n^{(2I)}$ and $a_n^{(2R)}$ and use the Borel dispersion relations to find instanton contributions to the imaginary part.

A ratio test on the weak-field coefficients of the 1-PI integral shows that they scale as

$$a_n^{(2I)} \sim 8.0\,(-1)^n\,\frac{\Gamma(2n+2)}{\pi^{2n+2}}\,. \tag{156}$$

The weak-field coefficients of the 1-PR integral reveal that, unlike $a_n^{(2I)}$, $a_n^{(2R)}$ scale as

$$a_n^{(2R)} \sim 0.1\,(-1)^n\,\frac{\Gamma(2n+3)}{\pi^{2n+3}}\,. \tag{157}$$

The results of the ratio tests on $a_n^{(2I)}$ and $a_n^{(2R)}$ are tabulated in tables. 1 and 2. Clearly, the growth is factorial, supporting the asymptotic analysis above. Using the Borel dispersion relation in eq. (136), the first instanton contributions to the imaginary parts of the 1-PI and 1-PR diagrams are given by

$$\operatorname{Im} \mathscr{L}^{(2)}_{\text{1-PI}} \sim \frac{q^2 m^4}{256\pi^4} (-ig_E)^4 \frac{-8.0\, i\pi}{2(ig_E)^2} e^{-\pi/g_E} , \tag{158a}$$

$$\operatorname{Im} \mathscr{L}^{(2)}_{\text{1-PR}} \sim \frac{q^2 m^4}{1024\pi^4} (-ig_E)^6 \frac{0.1\pi}{2(ig_E)^3} e^{-\pi/g_E} \tag{158b}$$

We have plotted the first instanton contributions in comparison to the Padé-Borel reconstructed imaginary parts in figs. . We notice that while the first instanton contribution provides a good approximation for the imaginary part of the 1-PI EHL, this is not the case for the first instanton contribution to the 1-PR diagram, as it is not able to capture the kink in the plot of the 1-PR plot. This points to a subdominant correction to the first instanton contribution in the 1-PR case. It was pointed out recently by Dunne [13] that such instanton correction corrections also appear in the 2-loop EHL for QED as an artifact of the loss of meromorphic properties at the order of 2-loops. To investigate this subdominant correction, we model the correction to the large order behaviour of $a_n^{(2R)}$ to be of the form

$$a_n^{(2R)} \sim 0.1(-1)^n \frac{\Gamma(2n+3)}{\pi^{2n+3}} + (-1)^n C \frac{\Gamma(2n+k)}{\pi^{2n+k}} \quad , \quad n \to \infty , \tag{159}$$

assuming $k < 3$. This sub-leading correction to the large order behaviour of the weak-field

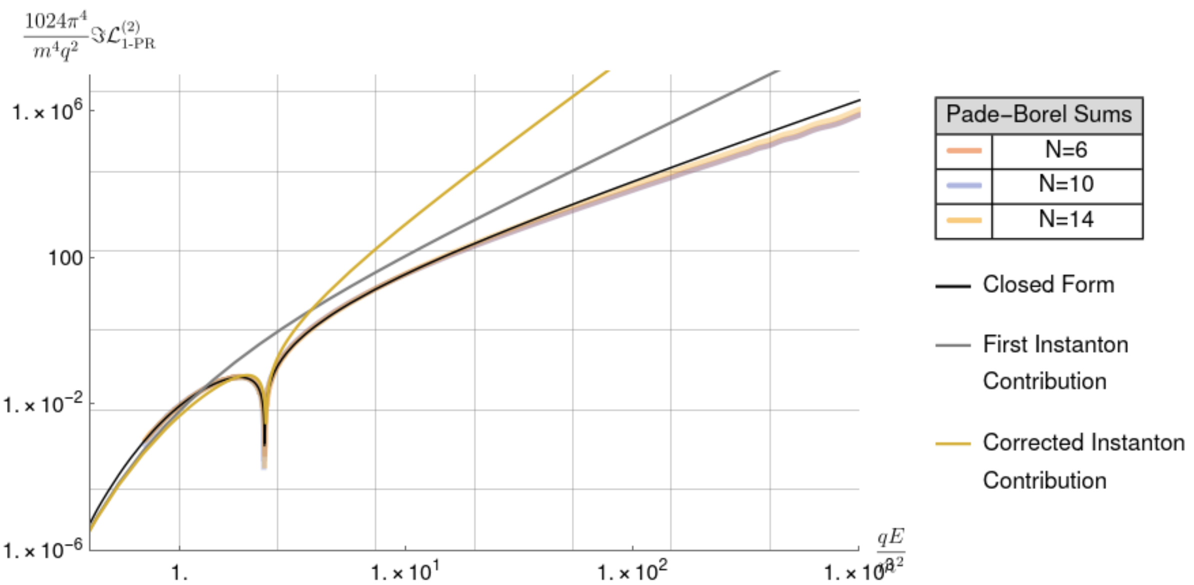

Figure 13: Padé-Borel reconstruction and first instanton contribution to the imaginary part of the 2-loop 1-PR sQED EHL. While the uncorrected first instanton contribution is not very effective at giving an approximation to the imaginary part because of the kink at $g_E \sim 10$, adding a subdominant correction term helps fix this problem.

n	an^2+bn+c
$5-10$	$0.404191n^2+0.243097n+0.128455$
$10-15$	$0.404741n^2+0.232291n+0.181699$
$15-20$	$0.404984n^2+0.225143n+0.234264$
$20-25$	$0.405094n^2+0.220784n+0.277354$

Table 1: A tabulation of $a_n^{(2I)}/a_{n-1}^{(2I)}$ fits to a quadratic polynomial an^2+bn+c for different ranges of n. The left column depicts the ranges of n for which the ratio $a_n^{(2I)}/a_{n-1}^{(2I)}$ was calculated and fitted, and the right column depicts the fit obtained from these ranges of n. The values of the fit-parameters a and b are seen to converge and indicate the asymptotic factorial growth of the 1-PI coefficients $a_n^{(2I)} \sim \Gamma(2n+2)/\pi^{2n}$.

n	an^2+bn+c
$20-30$	$0.405136n^2+0.618621n-0.449305$
$30-40$	$0.405238n^2+0.612768n-0.364672$
$35-45$	$0.405254n^2+0.611527n-0.341554$
$40-50$	$0.405264n^2+0.610714n-0.324364$

Table 2: $a_n^{(2R)}/a_{n-1}^{(2R)}$ ratio fits to the quadratic polynomial an^2+bn+c. The values of the fit parameters a and b are again seen to converge, indicating the asymptotic factorial growth of the 1-PR coefficients $a_n^{(2R)} \sim \Gamma(2n+3)/\pi^{2n}$.

coefficients will consequently lead to a correction to the instanton of the form

$$\operatorname{Im} \mathscr{L}^{(2)}_{\text{1-PR}} \sim \frac{q^2m^4}{1024\pi^4}\, g_E^6 \left[-\frac{0.1 i\pi e^{-\pi/g_E}}{2g_E^3} + C\, \frac{i\pi e^{-\pi/g_E}}{2g_E^k} \right] . \tag{160}$$

This instanton correction, while suppressed in the regime of weak fields, can rapidly overtake the leading instanton contribution for sufficiently strong fields and can, in fact, reverse the sign of $\operatorname{Im} \mathscr{L}^{(2)}_{\text{1-PR}}$.

Upon fitting the corrected instanton contribution with the 1-PR closed form, we found that $k = 1.5$ and $C = 0.027$ provides a good fit. Notice that the change in the sign of the imaginary part of $\mathscr{L}^{(2)}$ (which is signified by the kink in the plot) has physical significance as well— it shows that while the 1-PR contribution to the sQED EHL hinders pair production in the weak field region, it starts facilitating pair production for field values of the order $g_E \sim 10$. It would be interesting to study the physical implications of this phenomenon.

3.3 1-loop QED EHL: Two field case

The 1-loop EHL for QED is given by [10]

$$\mathscr{L}^{(1)}_{\text{QED}}(q,\epsilon,\eta) = -\frac{1}{8\pi^2}\int_0^\infty \frac{dt}{t^3}\, e^{-m^2 t}\left[\frac{q^2t^2\epsilon\eta}{\tan(q\epsilon t)\tanh(q\eta t)} - 1 - \frac{q^2t^2(\eta^2-\epsilon^2)}{3}\right] \tag{161}$$

There is no closed form for this function. However, this function can be written as a convergent summation made of the cos integral and sin integral functions [26]–

$$\text{Re}\ \mathscr{L}^{(1)}_{\text{QED}} = -\frac{q^2\epsilon\eta}{4\pi^3}\sum_{k=1}^{\infty} R_k^{(\epsilon)} + R_k^{(\eta)}\ , \tag{162}$$

where $R_k^{(\epsilon)}$ and $R_k^{(\eta)}$ are given by

$$R_k^{(\eta)} = \frac{\coth(\pi k\epsilon/\eta)}{k}\left[\text{Ci}\left(\frac{k\pi m^2}{q\eta}\right)\cos\left(\frac{k\pi m^2}{q\eta}\right) + \text{Si}\left(\frac{k\pi m^2}{q\eta}\right)\sin\left(\frac{k\pi m^2}{q\eta}\right)\right] \tag{163a}$$

$$R_k^{(\epsilon)} = -\frac{\coth(\pi k\eta/\epsilon)}{2k}\left[\text{Ei}\left(-\frac{k\pi m^2}{q\epsilon}\right)\exp\left(\frac{k\pi m^2}{q\epsilon}\right) + \text{Ei}\left(\frac{k\pi m^2}{q\epsilon}\right)\exp\left(-\frac{k\pi m^2}{q\epsilon}\right)\right]\ , \tag{163b}$$

and

$$\text{Im}\ \mathscr{L}^{(1)}_{\text{QED}} = \frac{q^2\epsilon\eta}{8\pi^2}\sum_{k=1}^{\infty}\frac{1}{k}\coth\left(\frac{k\pi\eta}{\epsilon}\right)\exp\left(-\frac{k\pi m^2}{q\epsilon}\right)\ . \tag{164}$$

It has been shown [27] that the summation in eq. (162) can be truncated at a finite order and can provide an excellent approximation by adding the remainder term

$$\text{Re}\ \mathscr{L}^{(1)}_{\text{QED}} = -\frac{q^2\epsilon\eta}{4\pi^3}\left[\sum_{k=1}^{N_s-1} R_k^{(\epsilon)} + R_k^{(\eta)} - \frac{\epsilon^2+\eta^2}{2N_s^2}\right]\ . \tag{165}$$

We will use this special series sum in order to estimate the QED EHL and make a comparison to the Padé-Borel reconstructions in order to check their efficacy.

Padé-Borel reconstructions

To find the Borel transform of the weak field expansion in the limit $\epsilon,\eta \to 0$, we will gather together terms $\epsilon^{m_1}\eta^{m_2}$ such that $m_1+m_2 = n$ for all $n = 0,1,2,\ldots$. Therefore, the n^{th} term is always a homogenous polynomial in ϵ and η. Therefore, the n^{th} term of the weak-field expansion can also be expressed as

$$\mathscr{L}^{(1)}_{\text{QED}} \sim \frac{1}{8\pi^2}\sum_{n=0}^{\infty} a_n^{(1)} P_n(x)\eta^n\ , \tag{166}$$

where $x = \epsilon/\eta$ and $P_n(x) = 1 + p_1 x + \cdots + p_n x^n$. Since the value of the n^{th} term must converge to the value of the n^{th} term in the weak-field expansion of a purely magnetic field in the limit

$x \to 0$, the value of $a_n^{(1)}$ defined here must coincide with the weak-field coefficients of the pure-magnetic field case. Also, because the EHL $\mathscr{L}^{(1)}_{\text{QED}}$ is invariant under the transformation

$$\epsilon \to -i\eta \tag{167a}$$

$$\eta \to -i\epsilon\ , \tag{167b}$$

and because $\mathscr{L}^{(1)}_{\text{QED}}$ is an even function of both ϵ and η, we must have that

1. Only even n's have a finite contribution to the weak-field expansion.

2. $p_k = 0$ for odd k.

3. $p_k = i^n p_{n-k}$.

The first few weak-field terms are listed below ($q = m^2 = 1$).

1. $n = 4$: $-\frac{\eta^4}{45}(-1-5x^2-x^4)$

2. $n = 6$: $\frac{2\eta^6}{315}(-2-7x^2+7x^4+2x^6)$

3. $n = 8$: $\frac{8\eta^8}{945}(3+10x^2-7x^4+10x^6+3x^8)$

etc. Now, we can define the Borel sum as

$$\widehat{\mathscr{S}}^{(1Q)}_{p,N^*}(\eta,x) = \sum_{n=0}^{N^*} \frac{a_n^{(1)}}{(2n+p)!} P_n(x)\eta^{2n+p}\ , \tag{168}$$

($a_n^{(1)}$ is now redefined to be the coefficient of η^{2n+4}). A Padé approximant can be contructed out of this Borel sum keeping x as a fixed constant. After this, we define the Padé-Borel sum as

$$\text{PB}_{N,f,p}(\eta,x) = \eta^{-p}\int_0^\infty dt\ e^{-t} P^N_{N+f}[\widehat{\mathscr{S}}^{(1Q)}_{p,N^*}](\eta t,x)\ , \tag{169}$$

Now, the presence of the functions $\tan(x\eta t)$ and $\tanh(\eta t)$ in the integrand of eq. (161), we expect to have singularities in the form of simple poles on the integration contour in eq. (169). We must therefore rotate the integration contour off the real axis in order to get a finite result. We will rotate the contour as $t \to t(1+ri)$, where we call the parameter of rotation as r. This rotation will render an imaginary part to the integral. With this set-up, we can start comparing our Padé-Borel sum with the numerically computed EHL in eq. (161).

Using the definition of Padé-Borel resummation defined in eq. (169), we can reconstruct the two-variable EHL for different values of x.

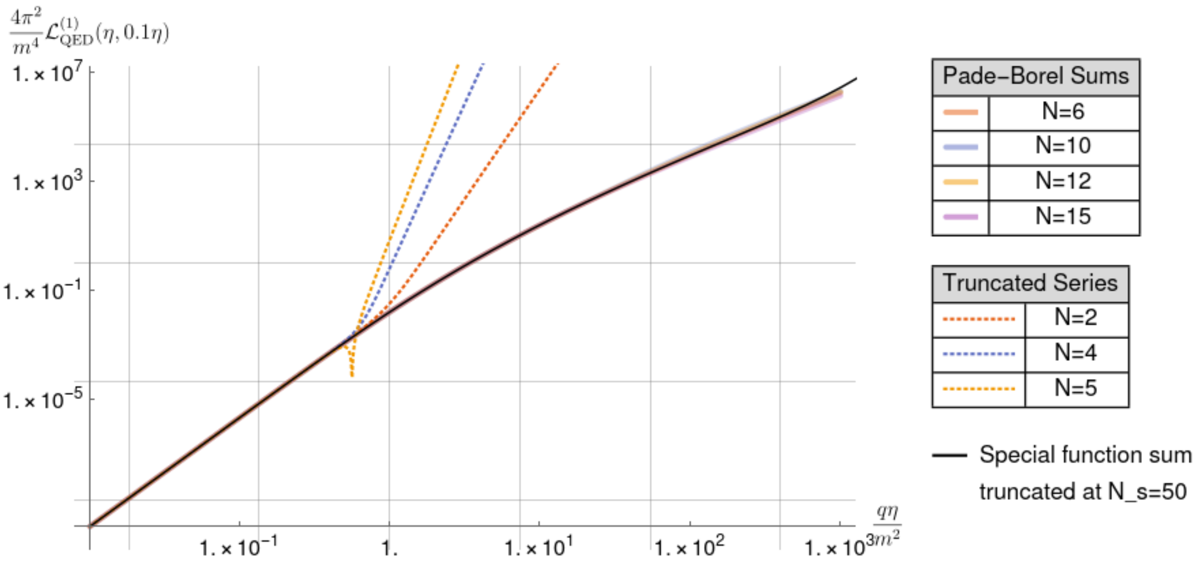

Figure 14: The Padé-Borel reconstruction for $x = 0.1$ with parameter values $p = 1$, $f = 1$ and the rotation parameter $r = 0.5$. The Padé-Borel summation is compared to the special function summation in eq. (165) truncated at $N_s = 50$. We see that the reconstruction does a very good job at approximating the QED EHL even for $N = 6$.

1. x = 0.1: In fig. 14, we have reconstructed the spinor EHL for $x = 0.1$ using the parameter values $p = 1$, $f = 1$ and compared it against the special functions sum in eq. (165) truncated at $N_s = 50$. Our Padé-Borel approximant provides a remarkably accurate estimate for the QED EHL even in the two-field case upto $g_\eta = q\eta/m^2 \sim 10^3$. We have again compared the reconstructions to the truncated asymptotic series, which diverges from the function at a very small value of g_η.

2. x=1 For $x = 1$, $\eta = \epsilon$. We have plotted the reconstruction for $x = 1$ in fig. 15. Clearly, the special function summation fails to converge even for $N_s = 500$ for large values of g_η. However, we see that the truncated special function estimation tends towards the Padé-Borel reconstruction in the strong-field regime. This indicates that the Padé-Borel reconstruction is in fact much more efficient at providing functional approximations to the two-field EHL than the convergent special function summation in eq. (165).

3. x=100 The Padé-Borel reconstruction not only works remarkably well for small values of x, indicating small field values, but also does astonishingly well for values of x as large as ~ 100. However, the reconstructions are only able to reproduce one of the kinks in the graph of fig. 16.

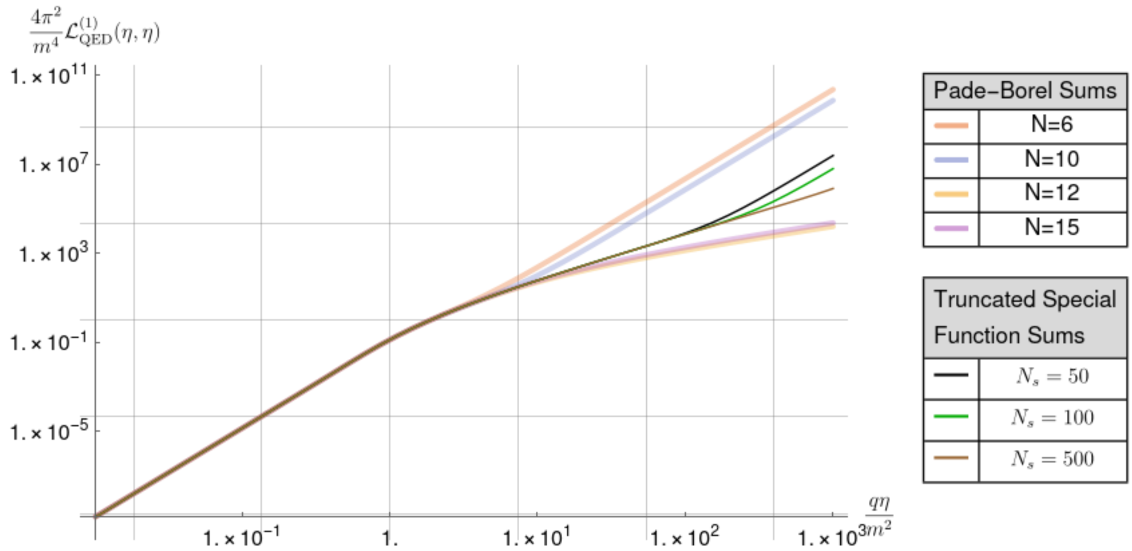

Figure 15: The Padé-Borel reconstruction for $x = 1$ with parameter values $p = 1$, $f = 1$ and the rotation parameter $r = 0.5$. The Padé-Borel summation is compared to the special function summation in eq. (165) truncated at different values of N_s. We see that although the truncated special summation and the reconstruction don't seem to agree in the strong field regime, the truncated special function sums seem to tend towards the higher-order Padé-Borel reconstructions for large values of N_s.

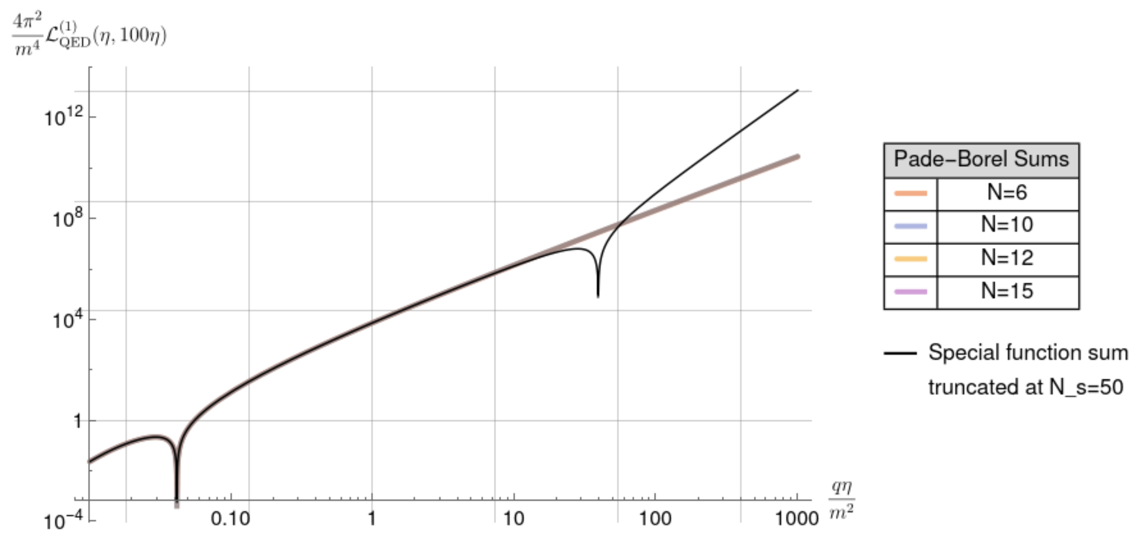

Figure 16: The Padé-Borel reconstruction for $x = 100$ with parameter values $p = 1$, $f = 1$ and the rotation parameter $r = 0.5$. Even for such a large value of x, the Padé-Borel reconstruction seems to reproduce the results from truncated special function sum quite well. However, it is not able to reproduce the second kink in the special function sum plot in the strong field regime.

4 Conclusions and Outlook

In this thesis, we have provided extensive proof of the remarkable ability of Padé-Borel recontructions to provide accurate functional approximations to the QED and sQED EHLs using very limited amount of asymptotic perturbative data. The fact that non-perturbative behaviour of a function in QFT can be predicted by just using a few terms in the perturbative expansion is astounding and can have far-reaching implications in the area of strong-field physics and is very relevant even today. The E-144, ELI-NP and LUXE experiments are working towards verifying QED at higher and higher laser intensities [28–32]. Calculations in such strong-field regimes could eventually require non-perturbative data upto the orders of many loops, which would inevitably require input from Resurgence strategies as the task of closed (or even integral) forms of contributions higher than 2-loops in four dimensions is impossible in the present day.

In Sec. 2 and , we derived integral forms of the 1-loop and 2-loop EHL for sQED, the results of which are encapsulated in eqs. (137), (122) and (127) . Subsequently, we calculated the perturbative coefficients from these integral forms and applied the method of Resurgence to these asymptotic series. We noticed many resurgent structures at one and two loops that have previously not been investigated in detail. In Sec. 3, we were able to successfully apply the method of Padé-Borel reconstruction to the 1-loop and 2-loop EHL for sQED for the single field case, both for magnetic and electric field backgrounds. In the reconstruction of the EHL in electric field backgrounds, we were also able to recover the non-perturbative imaginary part of the EHL which is responsible for Schwinger pair production even after only having knowledge of the perturbative data. We also showed that there is an ambiguity in the method of Padé-Borel reconstruction leading to a family of solutions that can be parametrized by f and p. To choose the correct solution from this family of solutions, we need to have some non-perturbative data regarding the large-order behaviour of the function. This data can easily be obtained from renormalization strategies [14]. Further, we also showed in this section that the Padé-Borel reconstruction strategy can in fact also be used for reconstructing the 1-loop EHL for QED in the case when both electric and magnetic fields are present. However, the analysis presented in this section will not be complete without the study of Resurgence and trans-series in this context. This is a future avenue of exploration full of possibilities.

This study was conducted with the objective of understanding resurgent structures and reconstruction strategies better so that such methods can be applied to physically relevant systems in the future. Already, these methods are being applied to quantum chromodynamics [33] and superconductivity [34]. In the context of QED, it may be possible to calculate non-perturbative contributions to the EHL upto the orders of several loops using Padé-Borel reconstruction strategies and design experiments to verify QED at higher and higher energy frontiers.

References

[1] C. M. Bender and S. A. Orszag, *Summation of Series*, in *Advanced Mathematical Methods for Scientists and Engineers I: Asymptotic Methods and Perturbation Theory*, (New York, NY), pp. 368–416, Springer New York, (1999).

[2] M. Mariño, *Instantons and Large N: An Introduction to Non-Perturbative Methods in Quantum Field Theory*, Cambridge University Press, (2015).

[3] F. J. Dyson, *Divergence of perturbation theory in quantum electrodynamics*, *Phys. Rev.* **85** (1952) 631.

[4] J. Ecalle, *Les fonctions résurgentes, vol. 1: Algébres de fonctions résurgentes*, *Publ. Math. Orsay* **81** (1981) .

[5] J. Ecalle, *Les fonctions résurgentes, vol. 2: Les fonctions résurgentes appliquées à l'itération*, *Publ. Math. Orsay* **81** (1981) .

[6] J. Ecalle, *Les fonctions résurgentes, vol. 3: L'équation du pont et la classification analytique des objets locaux*, *Publ. Math. Orsay* **85** (1985) .

[7] E. Borel, *Mémoire sur les séries divergentes*, *Ann. Sci. Éc. Norm. Supér* **16** (1899) 9.

[8] D. Dorigoni, *An Introduction to Resurgence, Trans-Series and Alien Calculus*, *Annals Phys.* **409** (2019) 167914 [1411.3585].

[9] D. Gupta and A. M. Thalapillil, *Resurgence in the Scalar Quantum Electrodynamics Euler-Heisenberg Lagrangian*, 2311.05688.

[10] W. Heisenberg and H. Euler, *Consequences of Dirac's theory of positrons*, *Z. Phys.* **98** (1936) 714 [physics/0605038].

[11] J. Schwinger, *On gauge invariance and vacuum polarization*, *Phys. Rev.* **82** (1951) 664.

[12] A. Florio, *Schwinger pair production from Padé-Borel reconstruction*, *Phys. Rev. D* **101** (2020) 013007 [1911.03489].

[13] G. V. Dunne and Z. Harris, *Higher-loop Euler-Heisenberg transseries structure*, *Phys. Rev. D* **103** (2021) 065015 [2101.10409].

[14] V. Weisskopf, *The electrodynamics of the vacuum based on the quantum theory of the electron*, *Kong. Dan. Vid. Sel. Mat. Fys. Med.* **14N6** (1936) 1.

[15] V. Ritus, *Lagrangian of an intense electromagnetic field and quantum electrodynamics at short distances*, *J. Exp. Theor. Phys.* **42** (1975) 774.

[16] V. Ritus, *Connection between strong-field quantum electrodynamics with short-distance quantum electrodynamics*, *J. Exp. Theor. Phys.* **46** (1977) 423.

[17] H. Gies and F. Karbstein, *An addendum to the heisenberg-euler effective action beyond one loop*, *Journal of High Energy Physics* **2017** (2017) 1.

[18] W. Dittrich and M. Reuter, *Effective Lagrangians in quantum electrodynamics*, no. 220 in Lecture notes in physics. Springer, Berlin, 1985.

[19] M. D. Schwartz, *Quantum Field Theory and the Standard Model*. Cambridge University Press, 3, 2014.

[20] S. L. Lebedev and V. I. Ritus, *Virial representation of the imaginary part of the Lagrange function of the electromagnetic field*, *Sov. Phys. JETP* **59** (1984) 237.

[21] G. V. Dunne, *Heisenberg-Euler effective Lagrangians: Basics and extensions*, in *From fields to strings: Circumnavigating theoretical physics. Ian Kogan memorial collection (3 volume set)*, M. Shifman, A. Vainshtein and J. Wheater, eds., pp. 445–522, (6, 2004), hep-th/0406216, DOI.

[22] R. S. Varga and A. J. Carpenter, *Zeros of the partial sums of cos(z) and sin(z).*, *Numerical Algorithms* **25** (2000) 363.

[23] I. E. Pritsker and R. S. Varga, *The szego curve, zero distribution and weighted approximation*, *Transactions of the American Mathematical Society* **349** (1997) 4085.

[24] A. CARPENTER, R. VARGA and J. WALDVOGEL, *Asymptotics for the zeros of the partial sums of e z . i*, *The Rocky Mountain Journal of Mathematics* **21** (1991) 99.

[25] N. Ahmadiniaz, J. P. Edwards and A. Ilderton, *Reducible contributions to quantum electrodynamics in external fields*, *Journal of High Energy Physics* **2019** (2019) .

[26] W. Mielniczuk, *The representation of the heisenberg-euler lagrangian by means of special functions*, *Journal of Physics A: Mathematical and General* **15** (1982) 2905.

[27] S. R. Valluri, D. R. Lamm and W. J. Mielniczuk, *Applications of the representation of the heisenberg–euler lagrangian by means of special functions*, *Canadian Journal of Physics* **71** (1993) 389 [https://doi.org/10.1139/p93-060].

[28] C. Bamber, S. J. Boege, T. Koffas, T. Kotseroglou, A. C. Melissinos, D. D. Meyerhofer et al., *Studies of nonlinear qed in collisions of 46.6 gev electrons with intense laser pulses*, *Phys. Rev. D* **60** (1999) 092004.

[29] C. Bula, K. T. McDonald, E. J. Prebys, C. Bamber, S. Boege, T. Kotseroglou et al., *Observation of nonlinear effects in compton scattering*, *Phys. Rev. Lett.* **76** (1996) 3116.

[30] D. L. Burke, R. C. Field, G. Horton-Smith, J. E. Spencer, D. Walz, S. C. Berridge et al., *Positron production in multiphoton light-by-light scattering*, *Phys. Rev. Lett.* **79** (1997) 1626.

[31] H. Abramowicz et al., *Letter of Intent for the LUXE Experiment*, 1909.00860.

[32] M. Pentia, C. R. Badita, D. Dumitriu, A. R. Ionescu and H. Petrascu, *The strong field qed approach of the vacuum interaction processes at eli-np*, 2023.

[33] R. Miravitllas Mas, *Asymptotic expansions, resurgence and large order behaviour of quantum chromodynamics*, Ph.D. thesis, Barcelona, Autonoma U., 2019.

[34] M. Mariño and T. Reis, *Resurgence for superconductors*, 1905.09569.